



universität
wien

DIPLOMARBEIT

Titel der Diplomarbeit

Influence of selected natural products on protein tyrosine
phosphatase 1B and insulin signalling

Verfasserin

Sophie Bartenstein

angestrebter akademischer Grad

Magistra der Pharmazie (Mag.pharm.)

Studienkennzahl lt. Studienblatt:

A 449

Studienrichtung lt. Studienblatt:

Diplomstudium Pharmazie

Betreuerin / Betreuer:

Univ.-Prof. Dr. Verena M. Dirsch

Wien, 2013

Abstract

With incidence of type 2 Diabetes mellitus (T2DM) and metabolic syndrome constantly rising, and current pharmacotherapy often being unable to achieve satisfactory results, a lot of effort is made in the search for new therapeutic options. Inhibition of protein tyrosine phosphatase (PTP) 1B, a major negative regulator of both the insulin and the leptin signalling pathway, has been found to be a promising strategy for the treatment of insulin resistance, a prominent feature of T2DM, and obesity.

In the course of the present work, fractions of extracts of plants traditionally used for the treatment of symptoms related to diabetes and metabolic disorders were tested for their PTP1B inhibitory activity in a colorimetric enzyme assay. Fractions that showed high activity were further tested for their ability to enhance insulin signalling in a cell based model using C2C12 myotubes. Several extracts were found to be highly active in the PTP1B enzyme assay and one fraction (*Leonurus sibiricus* fraction Ls 70a) also showed insulin-mimetic effects in the cell based system.

Furthermore, some common C18 fatty acids with different numbers, locations, and configurations of double bonds were tested for their inhibitory activity in the PTP1B enzyme assay. All tested fatty acids were able to inhibit PTP1B, with IC50 values in the micromolar range.

In order to establish an *in vitro* model for insulin resistance, C2C12 myotubes were treated with palmitate alone or in combination with TNF- α (to simulate inflammation). Palmitate treated cells showed lower insulin responsiveness than control cells, and TNF- α further increased insulin resistance. On mRNA level (but not on protein level), increased PTP1B expression in cells treated with palmitate and TNF- α was also detected.

Dysregulation of hypoxia inducible factor (HIF) 1 mediated transcription is also discussed to play a relevant role in the pathogenesis of T2DM and also of micro- and macrovascular diabetes complications. In this work some tests were conducted aiming to establish a luciferase reporter gene screening assay for HIF-1 activators under normoxic conditions: CHO cells were transfected successfully with the reporter and control plasmids, and dose-dependent induction of HIF-1-dependent luciferase expression by piperine was detected.

Zusammenfassung

Nachdem Typ 2 Diabetes mellitus (T2DM) und das metabolische Syndrom immer häufiger werden, und mit der derzeitigen Pharmakotherapie oft keine zufriedenstellenden Ergebnisse erreicht werden können, wird intensiv nach neuen Therapiemöglichkeiten gesucht. Die Hemmung der Protein Tyrosin Phosphatase (PTP) 1B, die sowohl die Insulin- als auch die Leptinsignaltransduktion hinunterreguliert, stellt eine vielversprechende Strategie für die Behandlung von Insulinresistenz, einem Hauptmerkmal von T2DM, und Adipositas dar.

Im Rahmen der vorliegenden Arbeit wurden Extraktfraktionen von Pflanzen, die in Asien traditionell für die Behandlung von Diabetes-assoziierten Symptomen und metabolischen Störungen eingesetzt werden, in einem colorimetrischen Enzymassay auf PTP1B-Hemmung getestet. Fraktionen mit hoher Aktivität wurden weiters in einem zellbasierten Testsystem mit C2C12 Myotuben auf ihre Fähigkeit getestet, die Insulinsignaltransduktion zu verstärken. Mehrere Extrakte hemmten PTP1B im Enzymassay sehr stark, und eine Fraktion (*Leonurus sibiricus* Fraktion Ls 70a) zeigte im Zellmodell insulinmimetische Wirkung.

Außerdem wurden einige weitverbreitete C18 Fettsäuren mit Doppelbindungen in verschiedener Anzahl, Position und Konfiguration im Enzymassay auf PTP1B-Hemmung getestet. Alle getesteten Fettsäuren waren aktiv, mit IC₅₀ Werten im mikromolaren Bereich.

Um ein *in vitro* Modell für Insulinresistenz zu entwickeln, wurden C2C12 Myotuben mit einer Palmitatlösung, allein oder in Kombination mit TNF α (um einen Entzündungszustand zu simulieren), inkubiert. Zellen, die mit Palmitat behandelt wurden, zeigten eine niedrigere Insulinantwort im Vergleich zu Kontrollzellen; TNF α verstärkte diese Insulinresistenz weiter. Auf mRNA-Ebene (aber nicht auf Protein-Ebene) war außerdem eine erhöhte Expression von PTP1B zu beobachten.

Dysregulation von Hypoxie-induziertem Faktor (HIF)-1 abhängiger Transkription scheint ebenfalls eine relevante Rolle in der Pathogenese des T2DM und außerdem der mikro- und makrovaskulären Diabeteskomplikationen zu spielen. Im Rahmen dieser Arbeit wurden einige Experimente durchgeführt mit dem Ziel, einen Screening Assay für HIF-1 Aktivatoren unter normoxischen Bedingungen zu etablieren. CHO-Zellen konnten erfolgreich mit dem Reporter- und dem Kontrollplasmid transfiziert und eine dosisabhängige Induktion der Luciferase-Expression durch Piperin gemessen werden.

Contents

1	Introduction	1
1.1	Outline of this work	1
1.2	Type 2 Diabetes mellitus	2
1.2.1	Definition and diagnosis of Diabetes mellitus	2
1.2.2	Pathogenesis and pathophysiology of T2DM	2
1.2.3	Treatment of T2DM	4
1.3	Insulin	6
1.3.1	General information	6
1.3.2	Insulin signal transduction	6
1.3.3	Insulin resistance	8
1.4	Protein tyrosine phosphatase 1B	9
1.4.1	Physiology	9
1.4.2	Regulation	10
1.4.3	PTP1B inhibitors for the treatment of T2DM	10
1.4.4	Plants/compounds tested for PTP1B inhibitory activity	11
1.5	Hypoxia inducible factor 1	13
1.5.1	General information	13
1.5.2	Regulation of HIF-1 transcriptional activity	14
1.5.3	HIF-1 and diabetes	15
1.5.4	Compounds tested for induction of HIF mediated signalling	16
2	Materials and Methods	19
2.1	Materials	19
2.1.1	Test extracts/compounds	19
2.1.2	Products and Supplier Information	21

2.1.3	Buffers and Solutions	26
2.1.4	Antibodies	34
2.2	Methods	35
2.2.1	PTP1B Enzyme Assay	35
2.2.2	Cell culture	38
2.2.3	Analyses on protein level	42
2.2.4	Analyses on mRNA level	45
2.2.5	Luciferase assay for induction of HIF-1 mediated transcription	47
3	Results and Discussion	53
3.1	PTP1B enzyme assay	53
3.1.1	Plant extracts	53
3.1.2	Fatty acids	56
3.2	Cell-based experiments related to PTP1B inhibition/insulin resistance	58
3.2.1	Establishment of the cell-based assay	58
3.2.2	Cell-based assays of plant extracts	59
3.2.3	Insulin resistance model	65
3.3	Cell-based experiments related to HIF-1 activation	70
3.3.1	Optimisation of transfection parameters	70
3.3.2	Luciferase assay	71
4	Summary and Conclusion	73
5	References	75
6	Appendix	91
	List of Tables	91
	List of Figures	91
	Abbreviations	93
	Curriculum Vitae	97
	Danksagung	99

1 Introduction

1.1 Outline of this work

Diabetes mellitus (DM) is one of the most common non-communicable diseases. Over the last years its prevalence has been and still is increasing significantly [1]. Diabetes is associated with reduced life expectancy and considerable morbidity, as well as reduced quality of life. Thus, it has a major impact on public health [2, 3]. With currently available antihyperglycemic drugs it is often not possible to adequately control glycemia and reduce the diabetes-associated cardiovascular risk, and patients suffer from adverse effects like weight gain and hypoglycemia [4]. Therefore, new ways to treat type 2 diabetes are sought for.

In this work, two promising targets for the future treatment of type 2 diabetes were addressed: protein tyrosine phosphatase (PTP) 1B and hypoxia inducible factor (HIF) 1. Fractions of extracts of several plants traditionally used in Asia against symptoms related to diabetes and the metabolic syndrome were tested for their PTP1B inhibitory activity in both an *in vitro* enzyme assay and a cell based model using C2C12 murine muscle cells. These assays were performed to possibly discover the molecular basis of the traditional use of these plants and to identify promising fractions for further bioassay-guided fractionation. Additionally, in some experiments C2C12 cells were treated with palmitate and TNF α , aiming to simulate the insulin resistant state *in vitro*, thus gaining more insight into the role and mechanism of PTP1B up-regulation in insulin resistance and obesity and potential susceptibility to the action of extracts/compounds of interest. Furthermore, a luciferase reporter gene assay to screen compounds or extracts for their ability to induce HIF-1 mediated transcription was established.

The screening for PTP1B inhibitors was performed as part of a project of

the Molecular targets group, Department of Pharmacognosy (University of Vienna) in cooperation with D. Steinmann and H. Stuppner (Institute of Pharmacy/ Pharmacognosy, University of Innsbruck) and S. Glasl (Department of Pharmacognosy, University of Vienna), who were responsible for the selection of plants as well as the extraction and fractionation steps.

1.2 Type 2 Diabetes mellitus

1.2.1 Definition and diagnosis of Diabetes mellitus

Diabetes mellitus (DM) is a general term for a group of metabolic diseases of diverse aetiology, all characterized by chronic hyperglycemia due to impaired insulin secretion and/or insulin action, leading to disturbances in carbohydrate, fat, and protein metabolism [5]. Diabetes is diagnosed if fasting plasma glucose concentrations exceed 7.0 mmol/l (126 mg/dl) or the 2-h plasma glucose level in the standardized oral glucose tolerance test is higher than 11.1 mmol/l (200 mg/dl)[2].

Two main types of DM are differentiated: type 1 or insulin-dependent DM and type 2 or non-insulin-dependent DM. Whereas in Type 1 DM destruction of the pancreatic β -cells leads to an absolute lack of insulin, in T2DM insulin production and secretion are often normal or increased until later disease stages, but the response of peripheral tissues (liver, skeletal muscle and adipose tissue) to the circulating insulin is impaired, leading to a relative lack of insulin and in consequence to elevated blood glucose levels [6].

According to estimates by the International Diabetes Federation, 366 million people worldwide suffered from DM in 2011. This number is thought to rise to 552 million by 2030 [1]. T2DM, largely caused by excess body weight and physical inactivity, makes up about 90 % of these cases [7].

1.2.2 Pathogenesis and pathophysiology of T2DM

T2DM is a multifactorial disease: genetic predisposition as well as environmental factors, such as high-caloric diet, sedentary lifestyle, and overweight, contribute to its pathogenesis [8]. Key features of T2DM include insulin resistance in liver

and muscle, and β -cell dysfunction (impaired insulin secretion) [9]. The interplay of these factors is summarized in Figure 1 [8].

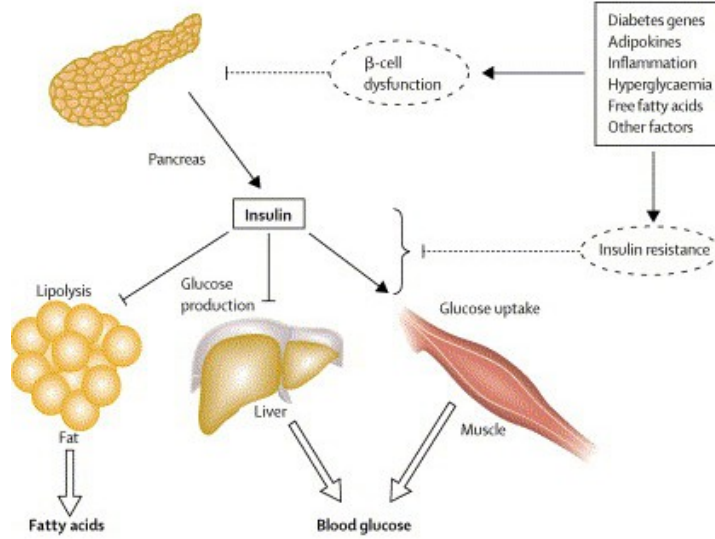


Figure 1: Pathology of T2DM: Various factors contribute to the development of insulin resistance and β -cell dysfunction, which together lead to increased lipolysis and glucose production (normally inhibited by insulin) in adipose tissue and liver, respectively, and decreased glucose uptake into the skeletal muscle (normally facilitated by insulin)(picture taken from [8]).

The development of T2DM begins with the development of insulin resistance in liver and skeletal muscle, present 10 to 20 years before the onset of diabetes [10], leading to increased hepatic glucose production and impaired glucose uptake into the muscle, and consequently postprandial hyperglycemia (see also section 1.3.3) [11]. Insulin resistance alone, however, does not determine the development of diabetes: Not all insulin resistant individuals develop hyperglycemia, as under normal conditions insulin secretion by the pancreatic β -cells can be increased sufficiently to compensate for the lack of insulin efficiency, and maintain normal glucose tolerance [12]. In some people, however, this compensation mechanism eventually fails, as β -cell function deteriorates and β -cell mass is lost over time. This leads to increased plasma glucose levels (both in postprandial and fasting state) and the onset of overt diabetes [11].

Long term complications of T2DM

Progressive worsening of hyperglycemia in T2DM leads to microvascular complications, such as neuropathy, retinopathy and nephropathy, as well as macrovascular complications like cardiovascular disease, stroke and peripheral vascular disease [3]. Cardiovascular disease is responsible for the majority of deaths caused by diabetes, which is the fourth or fifth leading cause of death in most high-income countries [1, 4].

1.2.3 Treatment of T2DM

Aims

As management of blood glucose levels was shown to reduce morbidity of T2DM patients, effective treatment of hyperglycemia is a primary objective in the treatment of T2DM. Other aims are the prevention of micro- and macrovascular complications, as well as the control of other features that often occur concomitantly with T2DM, namely dyslipidemia, hypertension, hypercoagulability, obesity, and insulin resistance (summarized in [13]).

Current treatment

At the diagnosis of T2DM, it is recommended to start treatment with lifestyle intervention (nutrition therapy and physical activity), potentially (depending on the severity of hyperglycemia) along with the initiation of pharmacotherapy with antihyperglycemic agents, usually metformin. Depending on blood glucose levels and percentage of glycated hemoglobin (HbA1c) that can be reached with this treatment, medication can be further adjusted by adding other antidiabetics or insulin to the regimen. The decision which antihyperglycemic drug(s) to choose for each patient is based on the characteristics of the patient (e.g. degree of hyperglycemia, risk of hypoglycemia, overweight/obesity, comorbidities) and of the agents (e.g. blood glucose lowering efficacy and durability, risk of inducing hypoglycemia, effect on weight, contraindications and side effects) [13, 14].

Currently available antihyperglycemic agents, their mechanisms of action, and some important characteristics are summarized in Table 1.

Table 1: Classes of antidiabetic agents, their mechanism of action, and some characteristics (based on [14])

Class (+examples)	Mechanism of action	Characteristics
Sulfonylureas (SU): Gliclazide, Glimepiride, Glyburide	stimulate endogenous insulin secretion by activation of SU receptor on pancreatic β -cells	effective lowering of blood glucose, weight gain, risk of hypoglycemia
Meglitinides: Nateglinide, Repaglinide	stimulate insulin secretion	frequent administration necessary (short half-life), less hypoglycemia than SUs
GLP-1 receptor agonists: Exenatide, Liraglutide	activate incretin pathway	improved postprandial control, weight loss, gastrointestinal side effects
DPP-4 inhibitors: Sitagliptin, Linagliptin	inhibition of dipeptidyl peptidase (DPP)-4 (inactivates GLP-1 and GIP)	improved postprandial control, weight neutral
Biguanides: Metformin	activation of AMP activated kinase leads to increased insulin sensitivity in peripheral tissues and liver	effective lowering of blood glucose, weight neutral, improved cardiovascular outcomes
Thiazolidinediones: Pioglitazone	activation of PPAR γ leads to increased insulin sensitivity in peripheral tissues and liver	good glycemic control, weight gain, risk of congestive heart failure; only if other treatment options (metformin) not suitable/successful [15]
α-Glucosidase inhibitors: Acarbose	inhibition of pancreatic α -amylase and intestinal α -glucosidase;	less effective in lowering glycemia than metformin and SUs; weight neutral, gastrointestinal side effects
Insulin: rapid-, short-, intermediate-, or long-acting	activation of insulin receptor	potentially greatest HbA1c reduction

Shortcomings and problems of current pharmacological treatment

While it is often possible to meet glycemic targets and reduce the incidence of microvascular complications with a combination of lifestyle intervention and currently available antihyperglycemic agents, even intensive treatment seems to have no beneficial effects on cardiovascular disease complications (summarized in [4, 13]). Moreover, current anti-hyperglycemic treatment often leads to weight gain, which in itself increases insulin resistance and the risk of cardiovascular morbidity, whereas weight loss can reduce hyperglycemia [16].

1.3 Insulin

1.3.1 General information

Insulin is a peptide hormone, produced by the pancreatic β -cells and secreted upon increase of the blood glucose concentration, which leads to increased glucose oxidation and a higher ATP:ADP ratio in the β -cell. This causes opening of ATP-controlled potassium channels in the cell membrane and consequent secretion of insulin.

Insulin stimulates the uptake of glucose, amino acids, and fatty acids into the major insulin responsive tissues (skeletal muscle and adipose tissue) and promotes the synthesis of glycogen, protein and lipids. Gluconeogenesis and glycogenolysis in the liver are inhibited. All in all, insulin action therefore results in the lowering of blood glucose levels [6, 17]. Apart from this metabolic effects, insulin also regulates cell growth and differentiation and modifies the expression and activity of enzymes and transport systems in various cell types [18, 19].

1.3.2 Insulin signal transduction

An overview over the insulin signalling pathway is given in Figure 2. Binding of insulin to its receptor (Insulin receptor, IR) – a protein tyrosine kinase receptor composed of two extracellular α - and two transmembrane β -subunits – leads to autophosphorylation of the β -subunits and activation of the receptor's tyrosine kinase activity. The receptor then phosphorylates adaptor proteins such as the insulin

receptor substrate-1 (IRS-1). This results in the recruitment of phosphoinositide-3-kinase (PI3K) to the plasma membrane and the subsequent phosphorylation of the protein kinase Akt, which in turn phosphorylates various substrates – among others the glycogen synthase kinase-3 (GSK3), which is thus inactivated, resulting in increased glycogen synthesis. Also, the insulin dependent glucose transporter GLUT4 is translocated to the plasma membrane, thus facilitating glucose influx into skeletal muscle and adipose tissue (reviewed in [17] and [20]).

Another pathway activated by insulin is the Ras-MAPK pathway, which accounts for the mitogenic effects caused by insulin: Grb2 and SOS bind to phosphotyrosine residues on insulin receptor substrate proteins, the small GTPase Ras and subsequently Raf are activated, triggering a kinase cascade that finally results in the phosphorylation and activation of ERK1/2 (extracellular signal-regulated kinases)(reviewed in [21]).

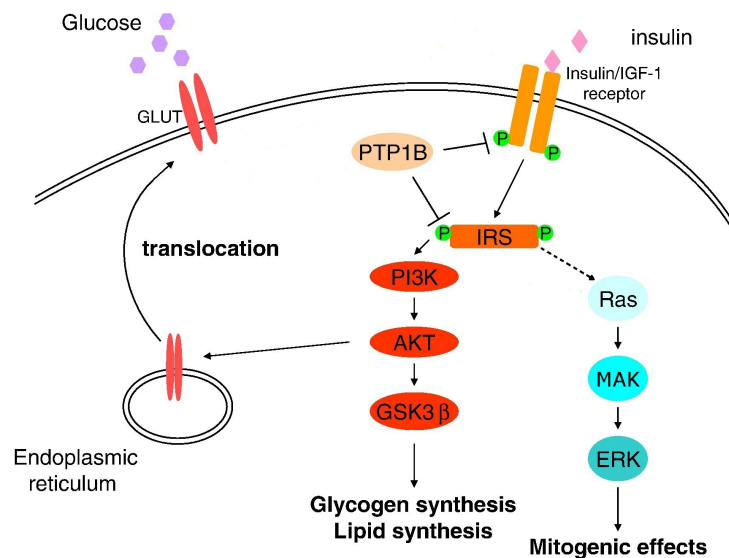


Figure 2: Overview of the insulin signalling pathway (modified from Liu et al.[22]): Upon insulin binding, the IR is autophosphorylated and activated. Adaptor proteins (e.g. IRS-1) are phosphorylated, PI3K is recruited to the cell membrane and phosphorylates Akt (activation), which in turn phosphorylates GSK-3 β (inactivation). As a result, glycogen synthesis and glucose uptake (translocation of GLUT4 to the cell membrane) are increased. Phosphorylation and activation of Ras, subsequently MEK, and finally ERK account for the mitogenic effects of insulin. PTP1B, by dephosphorylating the IR and IRS, is a major negative regulator of insulin signalling (see section 1.4).

1.3.3 Insulin resistance

Insulin resistance is a key feature of the metabolic syndrome and obesity, and plays a central role in the development of T2DM (cf. section 1.2.2) [23–25].

The term insulin resistance describes the impaired response of target tissues (liver, fat, muscle) to insulin [26]. It is a defect in insulin signal transduction [27]. The skeletal muscle, normally responsible for more than 75 % of all insulin-mediated glucose disposal, is the main site of insulin resistance in T2DM [25, 28].

Insulin resistance leads to reduced glucose uptake into muscle and adipose tissue, reduced glucose oxidation and glycogen synthesis in the skeletal muscle, increased release of free fatty acids (FFA) from adipose tissue into the circulation (due to impaired inhibition of triglyceride lipolysis), and increased hepatic gluconeogenesis [28, 29]

The etiology of insulin resistance can not be explained easily and is still incompletely understood [30]. Genetic predisposition as well as environmental factors such as excess caloric intake, physical inactivity, and obesity, and also infections, contribute to the development of insulin resistance [25, 27, 31].

On a molecular basis, elevated levels of circulating glucose, insulin, free fatty acids, and inflammatory cytokines (e.g. IL-1, IL-6, and TNF- α) seem to be the key factors leading to peripheral insulin resistance [27, 31]. In obesity, a low-grade inflammatory state, high amounts of inflammatory cytokines and FFAs are released from the expanded adipose tissue – this seems to be the link between obesity and insulin resistance (and ultimately T2DM) [12, 31]. Insulin resistance itself leads to increased plasma glucose, insulin, and FFA levels, which in turn further induce insulin resistance, leading to a vicious circle.

Insulin signal transduction can be impaired on all steps of the insulin signalling pathway (cf. Figure 2), including the IR itself (alterations in IR expression, insulin binding, phosphorylation state, and/or kinase activity). However, post-receptor defects (interruptions in proximal and/or downstream IR signalling events) are thought to be the primary reason for peripheral insulin resistance [27].

The kinase activity of the IR and the function of IRS proteins are tightly regu-

lated by their phosphorylation state. They are activated by tyrosine phosphorylation and inhibited by serine/threonine phosphorylation [17, 23, 32]. Increased activity and/or expression of protein tyrosine phosphatases (e.g. PTP1B, see section 1.4) or serine kinases can therefore lead to decreased insulin signalling.

These mechanisms have been suggested to underlie the induction of insulin resistance by FFAs and inflammation, too: High levels of plasma FFAs and TNF- α have been shown to activate serine kinases such as PKC (Protein kinase C; chronically activated in various models of insulin resistance) and IKK- β , and induce increased PTP1B expression [23, 27, 31, 33].

1.4 Protein tyrosine phosphatase 1B

1.4.1 Physiology

Reversible protein tyrosine phosphorylation is an important mechanism in the regulation of cell signalling [34]. Protein tyrosine phosphatases (PTPs) catalyze protein tyrosine dephosphorylation and are therefore able to modulate signal transduction pathways both in a negative or positive way [35, 36]. The ubiquitously expressed pTyr specific phosphatase PTP1B, belonging to the intracellular class of PTPs [37, 38], plays a major role in the regulation of insulin and leptin signalling [35]: Insulin signalling is negatively regulated by PTP1B by direct dephosphorylation of the activation segment of the IR [39] and of insulin receptor substrates (reviewed in [36]). Other examples for PTP1B substrates are JAK2 and STAT3 – this explains the modulating effect of PTP1B in the leptin signal transduction, which takes place via the JAK-STAT pathway [40, 41].

Although PTP1B dephosphorylates receptor tyrosine kinases and therefore can down-regulate their downstream signalling, PTP1B shows a positive effect on the activation of small GTPases, such as Ras, and their downstream MAPKs, which leads for example to ERK activation [42].

1.4.2 Regulation

The balance between protein tyrosine phosphorylation and dephosphorylation is important for the regulation of signal transduction pathways [34]. The activity of PTP1B is tightly controlled by location (PTP1B is targeted to the membrane of the endoplasmatic reticulum (ER) with its hydrophobic C-terminus [43]), oxidation, phosphorylation, sumoylation and proteolysis (reviewed in[44]). PTP1B, a major regulator of insulin signalling, is itself regulated by insulin action: Insulin binding to its receptor causes PTP1B phosphorylation in various positions, which can result in increased or decreased PTP1B activity (reviewed in[44]). Also, the Cys residue in the active site of PTP1B, which is essential for its catalytic activity, can be oxidized to a sulfenic acid by H_2O_2 , which is produced in response to insulin – this leads to reduced catalytic activity and an increased insulin response [45].

1.4.3 PTP1B inhibitors for the treatment of T2DM

As insulin resistance is a key feature in T2DM and metabolic syndrome, and PTP1B is a negative regulator of insulin signalling, it suggests itself that dysregulation of PTP1B plays a role in the pathogenesis of these diseases [46].

In several models for diabetes and obesity alterations in PTP1B expression and activity were observed, and mutations in the PTP1B gene leading to changes in expression and regulation of PTP1B, were shown to be associated with diabetes and obesity in humans [36, 46, 47]. PTP1B knock-out mice show increased insulin sensitivity compared to their PTP1B^{+/+} littermates and they are resistant to diet-induced diabetes and obesity [48]. Cell culture experiments showed that treatment with selective PTP1B inhibitors results in increased phosphorylation of IR β , IRS-1, Akt and ERK1/2, enhancing both basal and insulin-stimulated IR signalling [49]. Specific inhibition of PTP1B is therefore expected to enhance insulin and leptin sensitivity and seems a promising therapeutic strategy for the treatment of T2DM and obesity [38, 50].

As PTP1B acts as a negative regulator of receptor tyrosine kinases, concerns have been raised that inhibition of the enzyme might promote tumorigenesis. Indeed, PTP1B negatively regulates cell signalling in some cancer types, but in

others it has a positive signalling role in cell proliferation. So while PTP1B inhibition might promote tumour growth in the first cases, it might be a promising target to treat the latter (reviewed in [44]). PTP1B knock-out mice did not show increased tumour incidence [48], possibly because deletion of PTP1B leads to decreased activation of small GTPases (e.g. Ras) and their downstream MAPKs, and therefore to decreased mitogenic signalling [42].

Difficulties in PTP1B inhibitor development

The active site of PTP1B is highly charged and so are many of the inhibitors so far described (eg. vanadate). This leads to problems in bioavailability. Moreover, PTPs show a high degree of structural conservation of the active site, so inhibitor selectivity is a major issue in drug development [36]. Another thing that should be considered for the in vitro screening of potential inhibitors is the fact that the Cys residue in the active site of PTP1B is susceptible to oxidation – thus oxidizing agents might lead to false positive results [38].

1.4.4 Plants/compounds tested for PTP1B inhibitory activity

Leonurus sibiricus – Lamiaceae

Leonurus sibiricus (Honeyweed or Siberian motherwort) is used in traditional medical systems in Asia and South America as a drug against infections, inflammation, and diarrhoea, or as a tonic and general remedy [51–53]. Modern pharmacological studies have shown analgesic, anti-inflammatory and lipid-lowering effects [51, 53, 54].

Agrimonia pilosa – Rosaceae

Agrimoniae herba, the dried aerial parts of *Agrimonia pilosa* (Hairy agrimony), is prescribed in traditional chinese medicine (TCM) as adstringent, hemostatic, anti-diarrhoeal, cardi tonic or externally against eczema or furuncles [55, 56]. Activities proved so far include antiplatelet [57], antitumor [58], acetylcholinesterase inhibiting [59], antioxidant [60], anti-adipogenic [61], antinociceptive [62], anti-inflammatory [63], and antiviral effects [64].

Agrimonia pilosa is also traditionally used to treat diabetes and there are some studies that confirm blood-glucose lowering effects of the drug [65]. However, to date the mechanism of action of this antidiabetic effect has not been identified.

Terminalia species – Combretaceae

Various species of the *Terminalia* genus are traditionally used for medicinal purposes in the tropical region, where these deciduous trees are native. A high content in tannins is a common feature of the tested species (see below).

The fresh fruits, leaves and the bark of *Terminalia nigrovenulosa* are used as antidiarrhoeals in Thailand and Vietnam [66, 67]. Extracts of *T. nigrovenulosa* showed anti-cancer properties in vitro [67]. Gallic acid and 3,4-dihydroxybenzoic acid are prominent compounds found in *T. nigrovenulosa* extracts [67, 68].

Terminalia bellirica is used in traditional Indian medicine against infections, inflammations and gastrointestinal dysfunctions. It is also a component of ‘triphala’, an Ayurvedic herbal preparation used for example for the treatment of diabetes [69]. Extracts of *T. bellirica* showed blood glucose lowering, insulin sensitizing and obesity preventing effects in various animal models for (type 2) diabetes, both alone and in combination with *T. chebula* and *Phyllanthus emblica*, the other constituents of triphala [70–73]. Treatment with triphala was also shown to be able to reduce blood glucose levels in type 2 diabetic human subjects [74]. Octyl gallate was suggested as one of the active principles responsible for the antidiabetic properties of *T. bellirica* by stimulating insulin secretion [71].

Leaves of *Terminalia calamansanai* are used as a lithontriptic in Philippines [75]. The contained ellagitannins were shown to have cytotoxic effects [76].

Terminalia citrina is traditionally used in Thailand and India as antimicrobial, haemostyptic, against fevers, diarrhoea and other gastrointestinal dysfunctions, etc [69, 77]. In traditional Indian medicine, medicinal properties of *T. citrina* are thought to be similar to those of *T. chebula*, a constituent of ‘triphala’(see above) [69]. High antioxidant potential of extracts of *T. citrina* has been shown [77].

Tannins were isolated as major secondary metabolites in the fruit of *T. citrina* [78].

Fatty acids

As elevation of plasma free fatty acid levels is associated with T2DM and insulin resistance [79], it is surprising that oleic acid has been identified as the major PTP1B inhibitor in the bark of *Phellodendron amurense* and might therefore contribute to the blood glucose lowering effects of this herbal drug [80].

The impact of fatty acids on metabolic health is dependent on their length, saturation level and configuration: Dietary intake of saturated fatty acids (palmitic and stearic acid) is associated with an increased risk for the development of diabetes, while plasma levels of linoleic acid are inversely correlated with diabetes incidence [81]. The saturated fatty acids palmitate and stearate were shown to induce insulin resistance in cell models [82], whereas oleate can protect cells against palmitate induced insulin resistance [83, 84].

1.5 Hypoxia inducible factor 1

1.5.1 General information

Hypoxia inducible factors (HIF) are ubiquitously expressed heterodimeric transcription factors. They are central in the adaption of multicellular organisms to hypoxia (ie. reduced O₂ availability) both on systemic and cellular level and are indispensable for normal development. HIF target genes include genes involved in angiogenesis, apoptosis, cell cycle progression, glucose uptake, glycolysis and lipid metabolism. It consists of an α -subunit, HIF-1 α , and a β -subunit, HIF-1 β (also known as aryl hydrocarbon receptor nuclear translocator, ARNT), both of which belong to the family of basic helix-loop-helix transcription factors [85–88]. HIF-1 β is constitutively expressed in the nucleus, whereas HIF-1 α expression, protein stability, and activity are tightly regulated both oxygen-dependently and -independently, thus regulating the transcriptional activity of HIF-1 [86, 89].

Apart from HIF-1 α , other HIF- α -subunits, namely HIF-2 α and HIF-3 α , have

been identified, but have been less well studied so far. The β -subunit exists in several splice variants [90].

1.5.2 Regulation of HIF-1 transcriptional activity

As mentioned above, the transcriptional activity of HIF-1 is dependent on HIF-1 α protein level and activity [86].

Oxygen-dependent regulation of HIF-1 α level and activity

Under normoxic conditions HIF-1 α is hydroxylated by prolyl hydroxylases (prolyl hydroxylase domain proteins, PHDs), which results in the binding of the von Hippel-Lindau protein (VHL), subsequent ubiquitylation, and proteasomal degradation of the HIF-1 α protein [91]. The rate at which HIF-1 α is hydroxylated by PHDs is dependent on the cellular O₂ concentration – lower O₂ levels result in slower hydroxylation and therefore reduced degradation of HIF-1 α , leading to higher HIF-1 α levels in hypoxia. The active site of PHDs contains an Fe(II) ion, which can be chelated, or substituted by Co(II) – this results in inactivation of the enzyme, explaining why iron chelators (e.g. desferrioxamine) and CoCl₂ inhibit HIF-1 α degradation [91, 92].

Moreover, the HIF-1 α transactivation domain can be asparaginyl hydroxylated oxygen-dependently, for example by Factor Inhibiting HIF-1 (FIH-1), resulting in impaired coactivator binding [91].

Together, these two mechanisms lead to decreased HIF-1 transcriptional activity under normoxic compared to hypoxic conditions.

Oxygen-independent regulation of HIF-1 α level and activity

Besides the oxygen-dependent regulation of HIF-1 α -degradation via the VHL pathway, other, oxygen-independent, mechanisms to regulate HIF-1 α protein levels exist. Binding of the receptor of activated protein kinase C (RACK1) to HIF-1 α results in ubiquitylation and proteasomal degradation of HIF-1 α [93]. This pathway is modulated for example by the 90 kDa heat shock protein (HSP90), which competes with RACK1 for binding to HIF-1 α , and Calcineurin, which calcium-

independently phosphorylates RACK1 and thus inhibits the homodimerization necessary to induce HIF-1 α degradation [94, 95]. GSK3 β and forkhead box (FOX) O4, both of which are negatively regulated via the PI3K-Akt pathway, also promote VHL-independent HIF-1 α degradation [93, 96].

Not only HIF-1 α degradation is modulated via the PI3K-Akt pathway, but also its transactivation (FOXO3a, which is negatively regulated by Akt, inhibits HIF-1 α transcriptional activity), and its translation in response to growth factors and cytokines. The mammalian target of rapamycin (mTOR) and the MAPK pathways are also involved in the latter [93, 97].

1.5.3 HIF-1 and diabetes

Dysregulation of the HIF pathway has been shown to play a role in the pathophysiology of diseases including cancer, heart disease, pulmonary vascular disease, metabolic syndrome, and diabetes (reviewed in [87, 98]).

Disturbances in HIF-1 signalling have a detrimental role in several stages of the pathogenesis of T2DM, including insulin secretion, insulin resistance, adipocyte dysfunction and inflammation [88].

ARNT levels, and therefore HIF-1 transcriptional activity, are reduced in β -cells and liver of T2DM patients [88]. Slight increases in HIF-1 α protein levels, for example by administration of iron chelators like desferrioxamine, improve glucose stimulated insulin secretion, which is impaired in T2DM patients, in the pancreatic β -cells and lead to an up-regulation of IR and Akt in the liver [9, 88].

Mice lacking the HIF-1 α gene in hepatocytes show severe insulin resistance in skeletal muscle and adipose tissue, as well as reduction of hepatic glucose uptake after long-term exposure to a high fat/sucrose diet (HFSD). Conversely, HFSD results in reduced HIF-1 α protein levels and substantial increase of blood glucose levels in wild-type mice, suggesting down-regulation of HIF-1 α by hyperglycemia [99].

In the skeletal muscle, insulin induced up-regulation of glucose transporters was shown to be dependent on the HIF-1 α /ARNT transcriptional complex [100]. This suggests a role of HIF mediated signalling in insulin responsiveness in the skeletal muscle.

Adipose tissue of insulin resistant, obese subjects is hypoxic, and the consequent up-regulation of HIF-1 α leads to increased levels of inflammatory factors like IL-6 and leptin, suggesting a link between defects in adipocyte response to hypoxia and the development of insulin resistance and diabetes (reviewed in [88]). Inhibition of HIF-1 in adipocytes by adipose tissue specific knock-down of either HIF-1 α or ARNT protects mice from high fat diet-induced obesity and insulin resistance [101]. However, in experiments of a different group, transgenic mice expressing an adipocyte-specific dominant negative version of HIF-1 α were more susceptible to diet-induced obesity and insulin resistance than their wild-type littermates [102].

It was shown that global deletion of FIH, leading to a modestly increased HIF-1 transcriptional activity, protects mice against weight gain induced by high fat diet; mice on a normal diet showed increased energy expenditure and insulin sensitivity, weighed less and were smaller than wild type mice [103].

Overall, activation of HIF-1 α by small compounds may represent a viable approach to alleviate the dysfunctional metabolic control in T2DM.

HIF-1 signalling not only plays a role in the pathogenesis of T2DM itself, but also in the micro- and macrovascular complications linked to diabetes, where hypoxia is a key feature [88]. Hyperglycemia inhibits the hypoxia-induced stabilization of HIF-1 α protein and thus interferes with cell response to hypoxia [104]. HIF-1 α protein levels were severely reduced in wounds of leptin receptor-deficient mice compared with nondiabetic littermates – restoration of HIF-1 function accelerated wound healing [105], indicating a beneficial effect of HIF-1 α activation in for example diabetic foot ulcers.

1.5.4 Compounds tested for induction of HIF mediated signalling

CoCl₂

The inorganic compound CoCl₂ is well established as an activator of HIF-1 mediated transcriptional activity under normoxic conditions and is usually used in concentrations of about 100 μ M in cell culture experiments [106]. Exposing cells

to CoCl_2 causes induction of HIF-1 DNA binding activity and expression of downstream target genes, simulating the effects of hypoxia by augmenting the formation of reactive oxygen species and via the phosphatidylinositol-3-kinase and MAPK pathways [107–109].

Piperine

The piperidine alkaloid piperine is the main alkaloid in the fruits of *Piper nigrum* and their major pungent principle. Piperine has antioxidant properties and possesses bioavailability-enhancing activity [110].

Gingerol

Gingerol is one of the major pungent compounds in the rhizome of *Zingiber officinalis* and has antibacterial, anti-inflammatory and anti-tumour-promoting properties [110]. Gingerol was shown to increase HIF-1 α mRNA expression possibly by alleviating oxidative stress, in hypoxic mouse embryos, where HIF-1 α mRNA levels are usually decreased compared to embryos cultured in normoxic environment [111].

RTA and IM

RTA and IM are synthetic oleanane triterpenoids, synthesized at Dartmouth College, USA. Synthetic oleanane triterpenoids are multifunctional drugs, targeted at regulatory proteins controlling the activity of transcription factors (e.g. KEAP1, I κ B kinase,...) and thus affecting activities related to inflammation and the redox state of cells and tissues. This makes them potential drugs for the prevention and treatment of diseases with an inflammatory component [112].

2 Materials and Methods

2.1 Materials

2.1.1 Test extracts/compounds

The plant extracts tested in the course of this work were provided by cooperation partners at the Institute of Pharmacy/Pharmacognosy, University of Innsbruck, Austria and at the Department of Pharmacognosy, University of Vienna, Austria.

Plants were extracted with methanol on the ultrasonic bath, three times for 25 min. The extracts were then fractionated using a MPLC RP-18 column. These fractions were tested for their PTP1B inhibitory activity.

Table 2: Extracts and compounds tested for PTP1B inhibition or HIF1 α induction

Name	Concentration	Provider
<u>PTP1B inhibition:</u>		
Plant extracts:		
Subfractions of Agrimoniae herba pilosa (Ah)	10 $\mu\text{g}/\mu\text{l}$	D. Steinmann/ H. Stuppner (University of Innsbruck, Austria)
Subfractions of Terminalia nigrovenulosa herba (Tn)	10 $\mu\text{g}/\mu\text{l}$	D. Steinmann/ H. Stuppner (University of Innsbruck, Austria)

(continued on next page)

(continued from previous page)

Name	Concentration	Provider
Subfractions of Terminalia citrina herba (Tci)	10 µg/µl	D. Steinmann/ H. Stuppner (University of Innsbruck, Austria)
Subfractions of Terminalia bellirica herba (Tb)	10 µg/µl	D. Steinmann/ H. Stuppner (University of Innsbruck, Austria)
Subfractions of Terminalia calamansanai herba (Tca)	10 µg/µl	D. Steinmann/ H. Stuppner (University of Innsbruck, Austria)
Subfractions of Leonurus sibiricus leaves (Ls)	25 µg/µl	S. Glasl (University of Vienna, Austria)
Fatty acids:		
Stearic acid	1 µM to 30 µM	Sigma
Petroselinic acid	1 µM to 30 µM	Sigma
Oleic acid	1 µM to 30 µM	Sigma
Vaccenic acid	1 µM to 30 µM	Sigma
Linoleic acid	1 µM to 30 µM	Sigma
Linolenic acid	1 µM to 30 µM	Sigma
<u>HIF1α induction</u>		
CoCl ₂	100 µM and 200 µM	Sigma
Gingerol	3 µM and 10 µM	Sigma
Piperine	20 µM and 50 µM	Sigma

(continued on next page)

(continued from previous page)

Name	Concentration	Provider
RTA	0.03 μ M and 0.1 μ M	M. Sporn, Dartmouth Medical School, NH, USA
IM	0.03 μ M and 0.1 μ M	M. Sporn, Dartmouth Medical School, NH, USA

2.1.2 Products and Supplier Information

Table 3: Used products and supplier information

Name	Supplier
Enzyme	
PTP1B human recombinant enzyme	R&D Systems
<p><i>Lyophilized enzyme was solved to 1 μg/μl with PTP1B buffer and stored at -80°C in aliquots of 10 μl in small incubation tubes (long-term stock). For short-term storage the enzyme solution was split to 1.4 μl aliquots also stored at -80°C. Thus, repeated freeze/thaw cycles could be avoided. One aliquot of 1.4 μl was used per plate. Immediately before use it was diluted with 280 μl of cold PTP1B buffer to 0.005 μg/μl, then divided into two tubes. The tubes were kept on ice until and while the enzyme solution was pipetted into the wells (5 μl in a total assay volume of 100 μl).</i></p>	
Cell lines	
C2C12 murine myoblasts	ATCC
CHO	Michel Tremblay, McGill University, Montreal, Canada

(continued on next page)

(continued from previous page)

Name	Supplier
E.coli transformed with pGL3-EpoHRE-Luc	provided by Matthias Kramer, graduate student in the lab
Chemicals	
3-(N-morpholino)propanesulfonic acid (MOPS)	Sigma
para-Nitrophenylphosphate-disodium salt hex- ahydrate (pNPP)	Sigma
Dithiothreitol (DTT) <i>stored for use as a 1 M solution at -20°C</i>	Fluka
Ursolic acid (UA) <i>stored for use as 30 mM solution in DMSO at -20°C</i>	Sigma
Sodium ortho-vanadate (SOV) <i>stored for use as 10 mM solution in H_2O at -20°C</i>	Sigma
Dimethyl sulfoxide (DMSO)	Fluka
4-(2-hydroxyethyl)-1-piperazineethanesulfonic acid (HEPES)	Fluka
Ethylene glycol tetraacetic acid (EGTA)	Fluka
Ethylenediaminetetraacetic acid (EDTA)	Fluka
NaCl	Fluka
Na_2HPO_4	Fluka
KH_2PO_4	Fluka
Tris(hydroxymethyl)aminomethane hydrochlo- ride (Tris-HCl)	Sigma
Nonidet P40	Sigma
Sodium desoxycholal	Sigma
Sodium dodecyl sulfate (SDS)	Sigma

(continued on next page)

(continued from previous page)

Name	Supplier
NaN ₃	Sigma
Tetramethylethylenediamine (TEMED)	Fluka
Ammonium peroxy disulfate (APS)	Fluka
2-Amino-2-hydroxymethyl-propane-1,3-diol (Tris base)	Fluka
Glycine for electrophoresis (min. 99 %)	Sigma
Glycerol anhydrous	Fluka
Bromophenolblue	Sigma
Tween 20	Sigma
Luminol	Sigma
p-Coumaric acid	Sigma
H ₂ O ₂	Sigma
Sodium palmitate	Sigma
D-Luciferin (sodium salt)	Synchem
ATP	Sigma
Roti [®] -Quant	Carl Roth
Rotiphorese [®] 30 % acrylamide/bisacrylamide	Carl Roth
Bovine Serum Albumin	Sigma
Albumin V fraction fatty acid free	Sigma

Media and supplements

Dulbecco's Modified Eagle's Medium (DMEM)	Lonza
Fetal bovine serum (FBS)	Gibco, Invitrogen
Horse serum (HS)	Gibco, Invitrogen

Sera were heat inactivated at 56°C for 45 min and stored in aliquots at -20°C.

L-Glutamine	Lonza
Penicillin/Streptomycin mix	Lonza
LB broth	Sigma

(continued on next page)

(continued from previous page)

Name	Supplier
Ampicillin (sodium salt)	Sigma
Opti-MEM [®] Reduced Serum Medium	Invitrogen
Kits	
peqGOLD Total RNA Kit	peqlab Biotechnologie GmbH
peqGOLD DNase I Digest Kit	peqlab Biotechnologie GmbH
SuperScript [™] First-Strand Synthesis System for RT-PCR	Invitrogen
LightCycler [®] 480 SYBR Green I Master	Roche Applied Sciences
PureYield [™] Plasmid Midiprep System	Promega
Plasmids	
pEGFP-N1	Clontech
pGL3-EpoHRE-Luc (HIF-responsive element of erythropoietin promotor)	Prof. Kietzmann, University of Oulu, Finland
Primers for RT-PCR	
Mm_IL-6_1_SG QuantiTect Primer Assay (Actin)	Qiagen
Mm_Ptpn1.1_SG QuantiTect Primer Assay (PTP1B)	Qiagen
Mm_IL-6_1_SG QuantiTect Primer Assay (IL-6)	Qiagen
Miscellaneous material	
Luciferase lysis buffer	Promega
Trypsin	Invitrogen

(continued on next page)

(continued from previous page)

Name	Supplier
Recombinant human Tumor necrosis factor- α (hTNF α)	Sigma
Insulin	Sigma
Complete [™] protease inhibitor cocktail	Roche Diagnostics
Fugene [®]	Roche
Immun-Blot [™] PVDF Membrane (0.2 0.2 μ m)	BIO-RAD Laboratories
Precision Plus Protein [™] Standard	BIO-RAD Laboratories
Gel blotting paper	Whatman plc

Technical equipment

Eluator [™] Vacuum Elution Device	Promega
FACSCalibur [™] BD Biosciences	Pharmingen
LAS-3000 [™] Luminescent Image Analyzer	Fujifilm
Mini Trans-Blot [™] Electrophoretic Transfer Cell	BIO-RAD Laboratories
Power supply Power Pac [™] HC	BIO-RAD Laboratories
Tecan GENios Pro	Tecan
Tecan Sunrise	Tecan
Vac-Man [®] Laboratory Vacuum Manifold	Promega
Vi-Cell [™] XR Cell Viability Analyzer	Beckman Coulter
Light Cycler [®] 480 System	Roche Applied Sciences

Software

XFLUOR4 Version 4.51	Tecan
XFLUOR4GENIOSPRO Version 4.63	Tecan
Cell Quest Pro version 5.2	BD Biosciences
Vi-Cell [™] XR 2.03	Beckman Coulter
Image Reader LAS-3000 [™]	Fujifilm

(continued on next page)

(continued from previous page)

Name	Supplier
AIDA™ (Advanced Image Data Analyzer), version 4.06	Raytest GmbH
Excel	Microsoft
Light Cycler® 480 Instrument Software Version 1.5	Roche Applied Sciences

2.1.3 Buffers and Solutions

Table 4: Composition of buffers and solutions used for experimental procedures

Reagent/Solution	Amount
<u>PTP1B enzyme assay</u>	
MOPS buffer 50 mM:	
3-(N-morpholino)propanesulfonic acid (MOPS)	1046 mg
Aqua dest.	100 ml
NaOH	to pH 6.5
<i>stored at 4°C</i>	
Substrate solution: 4 mM pNPP in MOPS buffer (for one 96 well plate):	
para-Nitrophenylphosphate-disodium salt hexahydrate (pNPP)	11.14 mg
MOPS buffer	7.5 ml
Dithiothreitol (DTT) 1 M	15 µl
<i>prepared freshly for every experiment</i>	
PTP1B buffer:	
HEPES	10 mM

(continued on next page)

(continued from previous page)

Reagent/Solution	Amount
EGTA	0.1 mM
EDTA	0.1 mM
DTT	1 mM
BSA	0.5 mg/ml
<i>pH 7.5; stored in aliquots at -20°C</i>	
<u>Cell culture</u>	
Growth medium	
Dulbecco's Modified Eagle's Medium (DMEM)	500 ml
Fetal bovine serum (FBS)	10 %
L-Glutamine	2 mM
Penicillin/Streptomycin	100 U/ml /100 µg/ml
Differentiation medium	
DMEM	500 ml
Horse serum (HS)	2 %
L-Glutamine	2 mM
Penicillin/Streptomycin	100 U/ml /100 µg/ml
Starvation medium	
DMEM	500 ml
BSA	0.5 %
L-Glutamine	2 mM
Penicillin/Streptomycin	100 U/ml /100 µg/ml
Serum-free medium	
DMEM	500 ml

(continued on next page)

(continued from previous page)

Reagent/Solution	Amount
L-Glutamine	2 mM
Penicillin/Streptomycin	100 U/ml /100 µg/ml

Supplements/additives were sterile filtered into the bottle containing the medium.

Phosphate buffered saline (PBS)

NaCl	36.0 g
Na ₂ HPO ₄	7.4 g
KH ₂ PO ₄	2.15 g

pH 7.4; stored at 4°C after autoclaving

Trypsin/EDTA

Trypsin	0.05 %
Sodium EDTA	0.2 %
PBS	

Trypsin and EDTA dissolved in PBS, sterile filtered and stored in aliquots at −20°C

Sodium palmitate solution for insulin resistance model:

Sodium palmitate
Ethanol 96 %
Aqua dest.
Albumin V fraction fatty acid free

(continued on next page)

(continued from previous page)

Reagent/Solution	Amount
------------------	--------

Sodium palmitate was dissolved in a 1:1 mix of ethanol (96 %) and purified water by heating in heating block to 50°C to a concentration of 150 mM. This solution was diluted 1:20 with a 10 % solution of fatty acid free albumin in water and incubated for 60 min in a waterbath at 37°C while shaking to couple palmitate to albumin. The solution was then sterile filtered and stored in aliquots at -20°C.

Control solution for insulin resistance model:

Ethanol 96 %

Aqua dest.

Albumin V fraction fatty acid free

A 1:1 mix of ethanol (96 %) and purified water was diluted 1:20 with a 10 % solution of fatty acid free albumin in water and incubated for 60 min in a waterbath at 37°C while shaking. The solution was then sterile filtered and stored in aliquots at -20°C.

Protein extraction and determination

RIPA buffer

Tris (hydroxymethyl) aminomethane-hydrochloride (Tris-HCl) pH 7.4	50 mM
NaCl	500 mM
Nonidet P40	1 %
Na-desoxycholat	0.5 %
SDS	0.1 %
NaN ₃	0.05 %
Aqua dest.	

Immediately prior to use Complete™ was added

(continued on next page)

(continued from previous page)

Reagent/Solution	Amount
Bradford reagent	
Roti [®] -Quant	1 part
Aqua dest.	2.75 parts
<i>volume needed for 1 well: 190 μl</i>	

Sodium dodecyl sulfate polyacrylamide gel electrophoresis (SDS-PAGE)

APS – 10 % solution:

APS	1 g
Aqua dest.	ad 10 ml

stored at 4 °C

1.5 M Tris-HCl pH 8.8:

Tris-HCl	23.6 g
Aqua dest.	ad 100 ml
NaOH	to adjust pH

stored at 4 °C

1.25 M Tris-HCl pH 6.8

Tris-HCl	19.7 g
Aqua dest.	ad 100 ml
NaOH	to adjust pH

stored at 4 °C

Sodium dodecyl sulfate (SDS) – 10 % solution:

Sodium dodecyl sulfate (SDS)	10 g
Aqua dest.	ad 100 ml

stored at room temperature to avoid precipitation

(continued on next page)

(continued from previous page)

Reagent/Solution	Amount
Resolving gel (10 % polyacrylamide) – for 1 gel:	
30 % acrylamide/bisacrylamide	2.5 ml
1.5 M Tris-HCl pH 8.8	1.875 ml
10 % SDS	75 µl
Aqua bidest.	3.05 ml
TEMED	7.5 µl
10 % APS	37.5 µl
<i>Total volume: 7.5 ml</i>	
Stacking gel – for 1 gel:	
30 % acrylamide/bisacrylamide	640 µl
1.25 M Tris-HCl pH 6.8	375 µl
10 % SDS	37.5 µl
Aqua bidest.	2.62 ml
TEMED	7.5 µl
10 % APS	37.5 µl
<i>Total volume: 3.75 ml</i>	

(continued on next page)

(continued from previous page)

Reagent/Solution	Amount
------------------	--------

Preparation of Gel: All components for resolving gels were mixed in a Falcon tube, TEMED and APS being added last, thus starting the polymerisation of the acrylamide. The mixture was then poured into the gel holder, and approximately 2 ml of isopropanol were put on top to create an even layer of the gel and avoid evaporation. After about 20 min the resolving gel was fully polymerized. The isopropanol was then removed and the surface of the gel was briefly rinsed with Aqua dest. The mixture for the stacking gel was prepared in the same way and was poured on top of the resolving gel into the gel holder, at last putting in the comb to form wells.

When the stacking gel was polymerized, too, the gel was ready for gel electrophoresis. If not used immediately, gels were wrapped in wet paper tissues, put in a plastic bag, and kept in the fridge for up to a few days.

Electrophoresis buffer 10x:

Tris-(hydroxymethyl) aminomethane (Tris-base)	30 g
Glycine for electrophoresis (min 99 %)	144 g
SDS	10 g
Aqua dest.	ad 1000 ml

Stored at 4°C

Electrophoresis buffer 1x:

Electrophoresis buffer 10x	100 ml
Aqua dest.	ad 100 ml

SDS sample buffer 3x

0.5 M Tris-HCl pH 6.8	37.5 ml
SDS	6.0 g
Glycerol anhydrous	30.0 ml

(continued on next page)

(continued from previous page)

Reagent/Solution	Amount
Bromophenolblue	15.0 mg
Aqua dest.	ad 100 ml

10 mM DTT added prior to use. This 3x solution was mixed 1:3 with cell lysates (i.e. 1 part sample buffer, 2 parts lysate)

Western blotting and Immunodetection

Blotting buffer 5x:

Tris-base	15.169 g
Glycine	72.9 g
Aqua dest.	ad 1000 ml

Stored at 4°C

Blotting buffer 1x:

Blotting buffer 5x	200 ml
Methanol	200 ml
Aqua dest.	ad 1000 ml

Tris-buffered Saline Tween-20 (TBS-T) pH 8.0:

Tris-base	3.0 g
NaCl	11.1 g
Tween 20	1 ml
Aqua dest.	ad 1000 ml
HCl conc.	to adjust pH

stored at 4°C

Enhanced Chemiluminescence Reagent :

Aqua dest.	4.5 ml
1 M Tris-base pH 8.5	0.5 ml

(continued on next page)

(continued from previous page)

Reagent/Solution	Amount
Luminol (0.25 M in DMSO)	12.5 μ l
p-Coumaric acid (90 mM in DMSO)	11 μ l
30 % H_2O_2	1.5 μ l

H_2O_2 is added last.

Membrane stripping solution:

0.5 M NaOH

Blocking solution:

Bovine serum albumine (BSA)	2.5 g
TBS-T	ad 50 ml

2.1.4 Antibodies

Table 5: Antibodies used for Immunodetection

Target	Source	Molecular weight	Supplier
Primary antibodies:			
Phospho-Akt(Ser473)	rabbit	60 kDa	Cell signaling
Phospho-Insulin Receptor β (Tyr1361) (84B2)	rabbit	95 kDa	Cell signaling
Phospho-IGF-I Receptor β (Tyr1131)/Insulin Receptor β (Tyr1146)	rabbit	95 kDa	Cell signaling
Phospho-IGF-I Receptor β (Tyr1135/1136)/Insulin Receptor β (Tyr1150/1151) (19H7)	rabbit	95 kDa	Cell signaling
Insulin Receptor β (4B8)	rabbit	95 kDa	Cell signaling

(continued on next page)

(continued from previous page)

Target	Source	Molecular weight	Supplier
Phospho-p44/42 MAPK (Erk1/2) (Thr202/Tyr204)	rabbit	42/44 kDa	Cell signaling
Phospho-Gsk3 β (Ser9) (5B3)	rabbit	46 kDa	Cell signaling
I κ B α	rabbit	41 kDa	Cell signaling
α/β Tubulin	rabbit	55 kDa	Cell signaling
Purified mouse Anti-PTP1B	mouse	50 kDa	BD transduction laboratories
Secondary antibodies:			
anti Rabbit IgG	goat		New England Biolabs
anti Mouse IgG	goat		Upstate

All antibodies were used in a dilution of 1:1000 in TBS-T. Dilutions were stored at -20°C .

2.2 Methods

2.2.1 PTP1B Enzyme Assay

Principle

Extracts were tested for their PTP1B inhibitory activity using a colorimetric assay adapted by R. Baumgartner [113]. pNPP was used as a colorogenic substrate. Phosphatases dephosphorylate the colourless pNPP to the yellowish para-nitrophenol, addition of NaOH results in formation of para-nitrophenolate and an increase in optical density at a wavelength of 405 nm (Fig. 3 on the following page).

In presence of a phosphatase inhibitor, depending on its inhibitory activity, this reaction does not take place to the same extent and the measured absorption at 405 nm is lower.

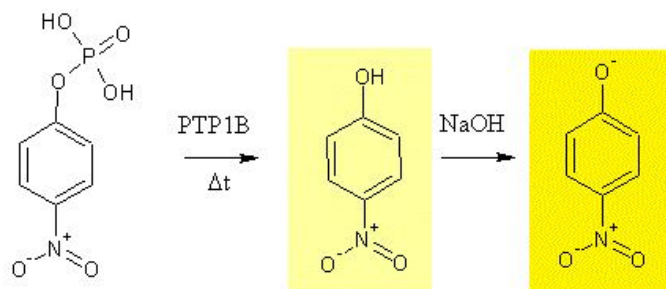


Figure 3: Mechanism of the chemical reaction resulting in the colour that is detected in the PTP1B enzyme assay.

Procedure

The PTP1B enzyme assay was carried out in 96 well microplates. Test compounds/extracts as well as positive controls (the known inhibitors ursolic acid [UA][114] and sodium orthovanadate [SOV][115]) were prediluted in DMSO to a concentration of 100 times the intended test concentration (cf. Table 2 on page 19), and then further diluted in MOPS buffer to 2 times the final concentration. For the blank, DMSO was diluted 1:50 in MOPS buffer, resulting in a final concentration of 1 %.

Extracts/compounds were tested in quadruplicate, both with and without enzyme.

Figure 4 on the facing page shows a pipetting scheme: 45 µl of the respective solutions were pipetted into rows A, B, E and F, and 50 µl into rows C, D, G and H. Then 50 µl of freshly prepared substrate solution (4 mM pNPP in MOPS buffer) were added to each well with a multichannel pipette. As pNPP is photosensitive, the microplate was covered from light while preparing further steps.

One vial of the prediluted enzyme (see page 21) was taken from the -80°C freezer and thawed by adding 280 µl of cold PTP1B buffer. The enzyme solution was mixed gently, half of it put into another, prechilled Eppendorf tube, thus making two aliquots. Then 5 µl of the enzyme solution (ie. 0.025 µg PTP1B) were added to each well in rows A, B, E and F, using the contents of the first tube for rows A and B, the contents of the second for rows E and F, always keeping the tube with the enzyme solution on ice. To minimize differences in measured total

enzyme activity throughout the plate, the pipetting process was carried out from left to right in rows A and E, and from right to left in row B and F (see Figure 4).

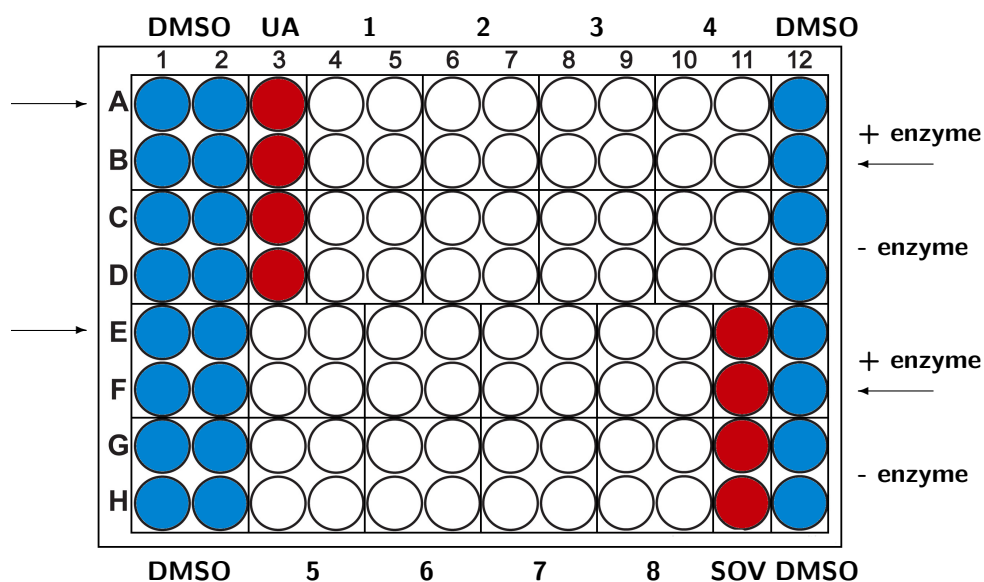


Figure 4: Pipetting scheme for PTP1B enzyme assay: A 96 well microplate was prepared with solutions of DMSO (indicated in blue), UA, SOV (red), and test extracts/compounds (1–8) and the substrate solution. Enzyme solution was added to rows A, B, E, and F, arrows indicate the direction in which the pipetting process was carried out.

After adding the enzyme, a kinetic measurement (11 cycles of 3 min, 5 sec of shaking and 2 sec of settling time before the measurement) of the absorbance at 405 nm was conducted with a Tecan Sunrise™ platereader. Then 25 µl of 10 M NaOH were added to each well to stop the reaction and ionize the reaction product, and an endpoint measurement of the optical density at 405 nm was conducted. This last value was used for the analysis of the experiment.

Analysis

The average of the absorbances (405 nm) of the DMSO wells without enzyme was subtracted from the average of the absorbances of the DMSO wells with enzyme. The resulting value was considered as corresponding to an enzyme activity of 100 %.

The average values of the wells with each test extract/compound without en-

zyme were also subtracted from the average values with enzyme – differences in absorption caused by the extracts themselves could thus be ruled out. The percentage of residual PTP1B activity was then calculated by normalizing the background corrected value for each extract/compound to the DMSO value.

If an extract/compound shows high inhibitory activity, the residual PTP1B activity is low, resulting in a low absorbance at 405 nm.

2.2.2 Cell culture

All cell culture procedures were carried out in a laminar airflow workbench. Media and reagents were prewarmed to 37 °C prior to use.

Cells were cultivated in the incubator at a temperature of 37 °C and a CO₂ concentration of 5 %.

Passaging of C2C12 and CHO cells

Cells were passaged every two to three days, at about 80 % confluence in a 1:10 ratio. The medium was removed, cells were briefly rinsed with prewarmed PBS to remove all traces of serum, then 3 ml of trypsin/EDTA were added and the tissue flask was incubated at 37 °C, 5 % CO₂ in the incubator until the cell layer was dispersed. 3 ml of fresh growth medium were added to terminate trypsinization, then the cell suspension was transferred to a 15 ml centrifuge tube and centrifuged at 200 g for 3 min. The supernatant was removed and cells resuspended in 10 ml growth medium. 1 ml of the suspension was transferred to a new 75 cm² tissue culture flask and another 10 ml of medium were added.

Seeding

C2C12 cells The rest of the cell suspension from the passaging step was filled with fresh growth medium to a total volume suitable to be divided on the wells/dishes required for the intended experiments. For example, for the analysis of extracts and insulin resistance experiments on protein level usually 24 ml of cell suspension were distributed to the wells of two 6-well plates (ie. 2 ml and approximately 300 000 cells per well). For experiments on mRNA level, 10 ml of cell

suspension were used for each 10 cm dish (approximately 1.5 million cells/plate).

CHO cells The rest of the cell suspension of the passaging step was diluted with fresh growth medium to a concentration of 0.25×10^6 cells/ml (cells counted using ViCell®) and 2 ml of this suspension were put into each well of a 6-well plate.

Differentiation of C2C12 cells

When cells on test plates reached confluence (about two days after seeding, depending on the density of the used cell suspension), growth medium was removed, wells were washed once with prewarmed PBS, and differentiation medium (2 ml per well of a 6 well plate, 10 ml per 10 cm dish) was added [116]. Every two days, medium was replaced with fresh differentiation medium, the grade of differentiation was assessed visually by light microscopy (cf. Fig. 5 and 6). All experiments using C2C12 cells were carried out with fully differentiated myotubes.

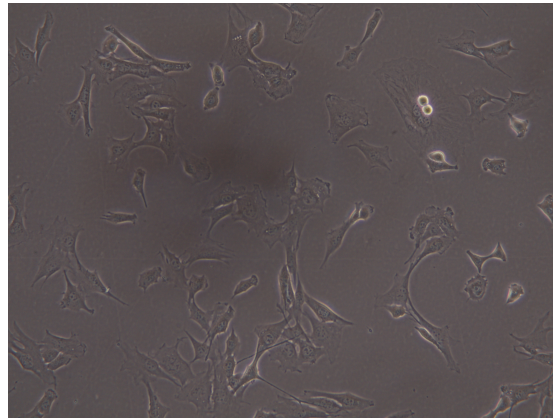


Figure 5: Undifferentiated C2C12 cells

Treatment of C2C12 cells for determination of suitable insulin concentration and stimulation time

Insulin concentration: C2C12 myotubes were serum starved for 3 h, pretreated with 5 μ M SOV for 30 min in order to enhance the signal for phosphorylated tyrosines and incubated with 0 nM, 10 nM, 30 nM, 100 nM, 300 nM and 1000 nM insulin for 5 min.

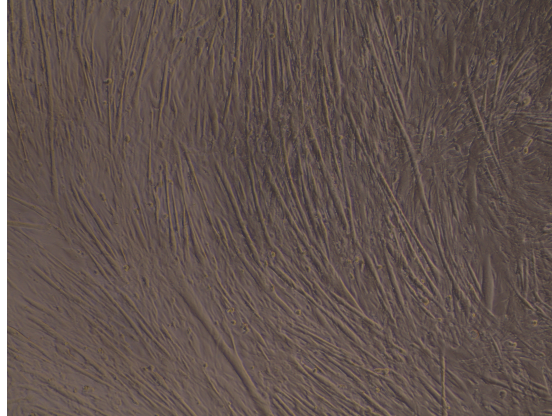


Figure 6: Fully differentiated C2C12 cells

Insulin stimulation time: C2C12 myotubes were serum starved for 3 h, pre-treated with 5 μ M SOV for 30 min in order to enhance the signal for phosphorylated tyrosines and then stimulated with 100 nM insulin for 0 min, 3 min, 10 min, 30 min, 45 min and 60 min.

Treatment of C2C12 cells for testing of extracts for PTP1B inhibition

For the PTP1B inhibition experiments, C2C12 cells were serum starved for a total of 3 hours to enhance insulin response [113]: Differentiation medium was removed, wells were washed once with prewarmed PBS and 2 ml of starvation medium per well were added. Cells were kept in the incubator at 37 °C.

135 min after the beginning of starvation, extracts were added to the media of two wells each. For the control, volumes of DMSO corresponding to the amount of extract were added to two wells (see Figure 7). DMSO concentrations never exceeded a final concentration of 0.3 %.

After addition of extracts, cells were incubated for 40 min, then 100 nM insulin were added to the media of one well per group (respective extract or control) and cells were incubated for further 5 min. To terminate insulin stimulation, plates were then put on ice, medium was removed, and wells were rinsed once with cold PBS.

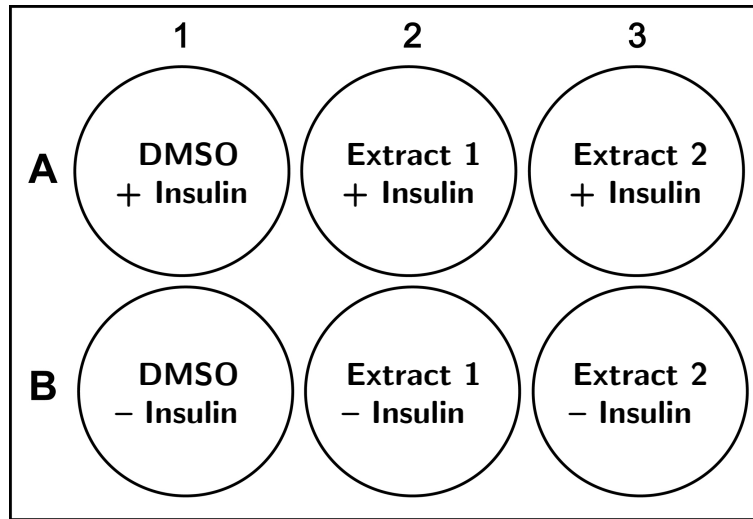


Figure 7: Pipetting scheme for the cell based testing of extracts for PTP1B inhibition: Extracts were added to the media in the wells of column 2 and 3 of a 6-well plate, corresponding amounts of DMSO were added to the wells of column 1 (control). Cells in row A were stimulated with 100 nM insulin (+ Insulin), cells in row B were left unstimulated (– Insulin).

Treatment of C2C12 cells for insulin resistance model

Differentiation medium was removed and wells/dishes were washed once with PBS.

For analyses on protein level, 2 ml of 1:10 dilutions of palmitate or control solution (preparation described on pages 28–29) in serum free medium were added to 4 or 2 wells of a 6-well plate, respectively. 10 ng/ml TNF α were added to 2 wells with palmitate containing media (see Figure 8). Plates were incubated for 18 h at 37°C, then medium was removed from wells that were to be stimulated with insulin, wells were washed with PBS and 2 ml of starvation medium were added to each well. Cells were starved for 3 h, then stimulated with 100 nM insulin for 5 min. To terminate insulin stimulation, plates were put on ice, the medium was removed, and wells were rinsed once with cold PBS.

For analyses on RNA level, 10 ml of 1:10 dilutions of the palmitate or control solution were used per 10 cm dish. In the experiments carried out so far, one sample dish with palmitate containing media, to which 10 ng/ml TNF α were added, and one control dish were prepared. Dishes were incubated for 21 h, then put on

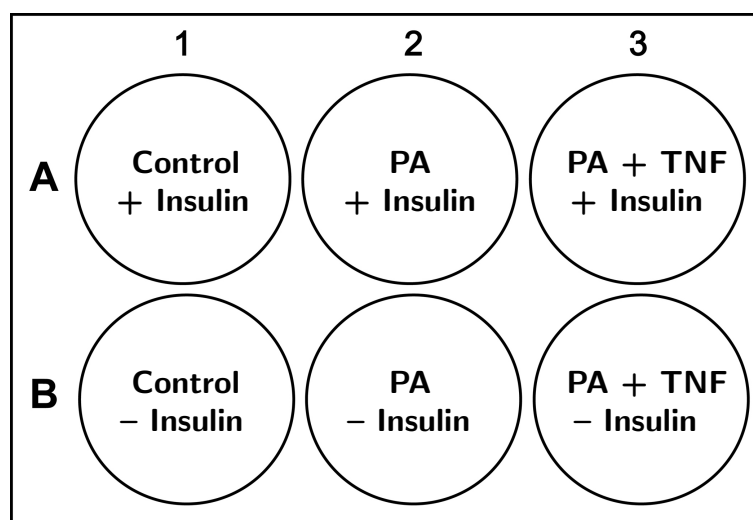


Figure 8: Pipetting scheme for insulin resistance experiments on protein level. Cells in column 1 were treated with the control solution, cells in column 2 with palmitate (PA) and cells in column 3 with both palmitate and TNF α (PA+TNF). Cells in row A were stimulated with 100 nM insulin (+ Insulin), cells in row B were left unstimulated (- Insulin).

ice and medium was aspirated.

2.2.3 Analyses on protein level

Protein extraction

150 μ l RIPA buffer containing Complete[™] Protease inhibitor cocktail were spread on the bottom of each well and plates were incubated for 5 min on ice. Cell lysates were transferred to 1.5 ml reaction tubes using a cell scraper and sonicated for 10 sec, while keeping the tubes on ice. Then lysates were centrifuged for 15 min at 13 000 rpm (16 060 g) at 4 °C. The supernatant was transferred to new reaction tubes and pellets were discarded.

Bradford Protein Determination

Aliquots of the protein extracts were used for protein determination, generally in a 1:10 or 1:15 dilution (depending on protein concentration). 10 μ l of the dilutions

were pipetted in triplicate into the wells of a 96 well plate. Triplicates of protein standard solutions (BSA in water, concentrations 0 µg/ml, 50 µg/ml, 150 µg/ml, 200 µg/ml, 300 µg/ml, 400 µg/ml and 500 µg/ml) were used to make a calibration curve. 190 µl of diluted Bradford reagent (cf. Table 4) were added to each well with a multichannel pipette, and absorption at 595 nm was measured using a Tecan Sunrise™ platereader.

Protein concentrations of the test solutions were calculated from the calibration curve using Microsoft Excel.

Gel electrophoresis

Sodium dodecyl sulfate polyacrylamide gel electrophoresis (SDS-PAGE) was used to separate the proteins of the cell extract by size. Migration speed in the gel is only dependent on the molecular weight of the protein, as any intrinsic charge is concealed by interaction of the negatively charged dodecyl sulfate molecules with the polypeptide chain [117]. In order to increase the sharpness of the protein bands, discontinuous gels were used (preparation of the gels described on pages 31–32).

Sample preparation: The amount of protein extracts corresponding to 30 µg protein was transferred to 1.5 ml Eppendorf tubes and mixed with half the volume of SDS sample buffer. This mixture was denaturated by heating it to 95 °C in a heating block for 5 min. As the sample buffer contains DTT as a reducing agent, disulfide bonds between polypeptide chains are broken during this process, thus destroying possible quaternary structures [117].

Samples were then spun down briefly to collect total volume at the bottom of the tube and kept on ice until loading of gel.

Electrophoresis: Electrophoresis was performed in a Biorad Minitrans-Blot® cell with 1x Electrophoresis buffer.

The denaturated protein samples were loaded into the wells of a 10 % Laemmli gel. Samples were run along with 5 µl of Precision Plus Protein™ Standard at 50 mA until molecular weight standard was fully separated and the first band

reached the bottom of the gel.

Western Blotting

Separated proteins were then transferred electrophoretically from the gel onto a methanol-activated PVDF membrane (100 V for 100 min). For this process, the used Biorad Minitrans-Blot[®] cell was filled with 1x Blotting buffer, and equipped with a freezer pack and a magnetic stirrer to keep the temperature in the chamber consistently low.

To prevent unspecific antibody binding membranes were then swayed in a solution of 5 % BSA in TBS-T for 1 hour to block free binding sites on the membrane.

Immunodetection

Incubation with specific antibodies: To detect target proteins on the western blotting membranes, the membranes were incubated overnight at 5 °C on a rolling shaker with a 1:1000 dilution of the specific primary antibody in TBS-T.

Membranes then were washed three times for 15 min with TBS-T on a horizontal shaker, incubated for 1 h at room temperature on a rolling shaker with a horse radish peroxidase (HRP)-linked secondary antibody (1:1000 in TBS-T) recognizing the primary antibody used before and again washed three times.

Development of the blots: In alkaline conditions and the presence of H₂O₂ the enzyme HRP coupled to the secondary antibody catalyses the oxidation of luminol to an excited form of 3-aminophthalate. The relaxation of the latter to ground level is accompanied by the emission of light [118, 119].

ECL (enhanced chemiluminescence) solution was freshly prepared (described on page 33) for each membrane, adding H₂O₂ last. TBS-T was removed from the membrane, ECL solution was added and the membrane was swayed for 30 to 60 sec in the ECL solution. Chemiluminescence was detected using a LAS-3000 image reader with automatic detection times provided by the software, using the high sensitivity-mode. The intensity of emitted light corresponds to the amount of target protein on the membrane.

2.2.4 Analyses on mRNA level

RNA isolation

For RNA isolation, C2C12 cells were grown in 10 cm dishes until confluence, and - when fully differentiated - treated with PA/TNF for 21 h (cf. section 2.2.2 on page 41).

RNA isolation was conducted using the peqGOLD Total RNA kit according to the manufacturer's instructions: Dishes were put on ice and medium was removed by aspiration. Further steps were conducted at room temperature. 800 µl of RNA Lysis Buffer T were added to each dish and dishes were incubated for 5 min at room temperature. Then cell layers were scratched from the bottom of the dish and the lysates transferred directly into the DNA removing columns placed in 2.0 ml collection tubes. Tubes with columns were centrifuged for about 8 min at 13 000 rpm (16 060 g). Flow-through lysate was transferred to a new 1.5 ml reaction tube and mixed with 800 µl of 70 % ethanol by vortexing. Lysate was pipetted on a PerfectBind RNA column placed in a collection tube, all centrifuged for 1 min at 13 000 rpm (16 060 g). Flow-through liquid was discarded, RNA now being bound to the columns.

After columns had been washed with 500 µl RNA Wash Buffer I by centrifuging for 15 sec, DNase digestion was carried out directly on the column. For each column DNase I digestion mix was prepared according to manufacturer's instruction, and 75 µl of the mix were pipetted directly on the resin of the column. The columns were incubated for 15 min at room temperature. Then 400 µl RNA Wash Buffer I were added, columns were incubated for 5 min and then centrifuged at 13 000 rpm (16 060 g) for 5 min – flow-through liquid is discarded. Next, columns were washed twice with 600 µl of RNA Wash Buffer II by centrifuging at 13 000 rpm (16 060 g) for 15 sec. Then columns were dried by centrifuging above an empty collection tube for 3 min at 13 000 rpm (16 060 g) until completely dry. 50 µl of 70 °C warm RNase-free water were then pipetted on the resin and the columns were incubated for 5 min at room temperature before RNA was eluted by centrifuging at 7000 rpm (4500 g) for 5 min.

Isolated total RNA was UV-spectroscopically quantified and kept at –80 °C until further use.

Agarose gel electrophoresis

To determine successful isolation of intact RNA, aliquots of the RNA extracts were mixed with gel-loading buffer and loaded on a 1 % agarose gel (agarose dissolved in 0.5 % Tris/Borate/EDTA buffer (TBE)). SYBR[®] Safe DNA stain was added to the gel in a concentration of 1:10 000. Gel was run at 150 V for 30 min, then the RNA bands were visualized in UV light. Two sharp bands (representing 18S and 28S rRNA) indicate a successful preparation of intact total RNA, while degraded RNA would have a smeared appearance [120].

Reverse transcription

For reverse transcription, the SuperScript[™] II First-Strand Synthesis System was used.

5 µg total RNA, 30 ng random hexamers, 1 µl dNTP mix (10 mM) and PCR grade water to a total of 12 µl were mixed and incubated for 5 min at 65 °C. Then the reaction tube was put on ice for 2 min and 2 µl 10x strand buffer, 2 µl DDT (0.1 M) and 1 µl RNase OUT inhibitor were added. The mix was incubated for 2 min at room temperature, before 1 µl of Superscript II RT Enzyme was added. Tubes were then incubated first for 10 min at room temperature, then for 90 min at 42 °C and finally for 15 min at 70 °C. 1 µl RNase H was then added and the mix was incubated for 20 min at 37 °C to digest the remaining RNA template.

The thus obtained cDNA was stored at –80 °C until use.

Quantitative Real Time PCR

qPCR was conducted for IL-6 and PTP1B as targets, actin was used as an endogenous control. For IL-6 and actin, cDNA was diluted 1:10 with PCR-grade water, for PTP1B undiluted cDNA-solution was used. qPCR was carried out in triplicate for every gene.

A mix of 7.5 µl SYBR Green I Master (2x conc), 1.5 µl Primer and 4.5 µl SYBR Green I Master H₂O PCR-grade was pipetted to each well and 1.5 µl cDNA solution (or PCR-grade water as negative control) were added.

PCR was run according to the protocol presented in Table 6 on the facing page.

Table 6: Protocol used for quantitative real time PCR

	Target (°C)	Acquisition Mode	Hold (mm:ss)	Ramp Rate (°C/s)
Denaturation	95	none	10:00	4.4
Cycles: 1; Analysis mode: none				
Amplification	95	none	00:05	4.4
	61	none	00:05	2.2
	72	single	00:15	4.4
Cycles: 60; Analysis mode: Quantification				
Melt	95	none	00:05	4.4
	60	none	00:10	2.2
	95	continuous		0.11
Cycles: 1; Analysis mode: Melting curve (acquisition every 5 °C)				

Analysis of qPCR: The relative expression levels of PTP1B and IL-6 of cells treated with PA+TNF were calculated using the ddCt method [121]. Actin was used as internal control (to normalize the PCRs for the amount of RNA that was reverse transcribed), untreated control cells (ie. cells treated with the control solution) were used as calibrator.

2.2.5 Luciferase assay for induction of HIF-1 mediated transcription

For luciferase assay, CHO cells were co-transfected with the reporter plasmid pGL3-EpoHRE-Luc and pEGFP-N1 (as internal control).

Binding of hypoxia inducible factor-1 (HIF-1) to hypoxia responsive elements (HRE) enhances transcription of the downstream genes [122]. In case of the pGL3-EpoHRE-Luc plasmid, HIF-1 binding results in the induction of luciferase (Luc) expression, the level of which can be measured in the luciferase reporter gene assay. Changes in HIF-1 transcriptional activity caused by treatment of cells with test substances (eg. by influencing the stability of HIF-1 α) will lead to changes in detected luminescence. pEGFP-N1 encodes for a variant of wild-type GFP (green fluorescent protein). Fluorescence of transfected cells is used to determine

transfection rate and to normalize luminescence to fluorescence for the analysis of luciferase assay, to ensure that higher measured luminescence is caused by higher luciferase expression per cell in contrast to higher numbers of viable cells.

Isolation of pGL3-EpoHRE-Luc plasmid

Pre-culture: 4 ml sterile LB-medium containing 100 µg/ml ampicillin were inoculated with 1 loop of the glycerol stock of the plasmid carrying E.coli stem and incubated at 37 °C in a shaking incubator (medium speed) until cloudiness of medium indicated good bacterial growth.

Main culture: The pre-culture was added to 200 ml of autoclaved LB-medium containing 100 µg/ml ampicillin in a sterile Erlenmeyer flask. The culture was incubated overnight at 37 °C in a shaking incubator (medium speed).

Plasmid isolation: From the main culture, the plasmid was isolated using the PureYield™ Plasmid Midiprep System according to the manufacturer's instructions.

Transfection

0.5 x 10⁶ CHO cells were seeded into each well of a 6-well plate. Plates were then incubated at 37 °C for 24 h before starting transfection.

A transfection mix of 100 µl Opti-MEM® (amount for 1 well of a 6-well plate), plasmid DNA and Fugene® HD was prepared in a sterile reaction tube and incubated at RT for 15 min. Different amounts of pEGFP plasmid and Fugene® were used to find out the right DNA:Fugene® ratio to achieve optimal transfection efficacy for the actual assay.

Medium from the wells where cells were to be transfected (some cells needed as untransfected controls) was replaced with 1 ml Opti-MEM®. The transfection mix was drop by drop added to the medium. After the plates had been kept at 37 °C for 4 h, 1 ml of growth medium was added to each well and cells were left in the incubator overnight.

Reseeding for luciferase assay

Medium was removed, cells were rinsed with prewarmed PBS and trypsinized with 1 ml trypsin/EDTA per well. When cells started to detach from the bottom of the wells, 1 ml growth medium was added to each well and cell suspensions were transferred to 15 ml centrifuge tubes, one for transfected and one for untransfected cells.

Cell suspensions were diluted to a concentration of 600 000 cells/ml (number of viable cells determined with a ViCell[®] cell counter) and 100 μ l of these suspensions (ie. 60 000 cells per well) were then pipetted into each well of a 96 well plate – the first column of the plate was seeded with untransfected (for background measurement), the rest with transfected cells. The plates were incubated for 60 min at 37 °C prior to treatment in order to allow cells to adhere to the plate.

About 1 ml of each cell suspension, transfected and untransfected, were put aside for a flow cytometric measurement of the transfection rate.

Measurement of transfection rate

Suspensions of transfected and untransfected control cells were transferred to flow cytometry sample tubes, spun down, supernatants were discarded and cells resuspended in 1.5 ml PBS.

Measurement was conducted with a BD FACSCalibur[™] flow cytometer. With the peak of untransfected cells being at 1 to 10 arbitrary fluorescence units, cells with an FL1-H (green fluorescence) value higher than 10 were considered as transfected successfully (green fluorescence caused by expression of EGFP). The transfection rate was calculated as the percentage of these cells.

Treatment

Test compounds (solved in DMSO) were diluted in growth medium to 2-times the desired final concentration. 100 μ l of these solutions were then added to the wells of a 96 well plate containing the transfected cells and 100 μ L growth medium (experiment was carried out in quadruplicate). Plates were incubated for 18 h at 37 °C, 5 % CO₂. 0.1 % DMSO (final concentration in growth medium) was used

as negative control.

Treatment was terminated by aspiration of the medium and the 96 well plates were immediately frozen at -80°C .

Luciferase reporter gene assay

Principle: In the luciferase assay, the chemiluminescence caused by the oxidation of luciferin to oxiluciferin is measured. This reaction is catalyzed by luciferase, with $\text{ATP} \cdot \text{Mg}^{2+}$ as cosubstrate [123].

Experimental procedure: Plates were taken out of the -80°C freezer and cells were lysed by adding 50 μl luciferase lysis buffer (containing 1 mM DTT) to each well and incubating the plates on a horizontal plate shaker for 10 min. Then 40 μl of the cell lysate were transferred to a black bottom 96-well plate using a multi-channel pipette. EGFP-derived fluorescence and luminiscence were measured with a Tecan GENios Pro. Measurement parameters are stated in Table 7 on the next page).

Analysis: Luminiscence values were normalized to the EGFP-derived fluorescence, in order to account for differences in cell number and transfection rate. The average of the four normalized luminiscence values of each set were then compared to the average of the normalized luminiscence values of the DMSO control.

Table 7: Tecan GENios Pro measurement parameters for Luciferase reporter gene assay

Parameter	Setting
EGFP-derived fluorescence measurement:	
Measurement mode	Fluorescence
Excitation wavelength	485 nm
Emission wavelength	520 nm
Gain	Optimal
Number of reads	1
Integration time	1000 μ s
Lag time	0 μ s
Mirror selection	40 ms
Luminiscence measurement:	
Measurement mode	Luminiscence
Integration time (manual)	2000 ms
Attenuation	none
Plate definition file	GRE96fb
Part of the plate	A1 - H 12
Time between move and integration	50 ms
Well kinetic number	1
Well kinetic intervall (minimal)	2020 ms
Injector A volume	50 μ l
Injector A speed	200 μ l/s
Injector B volume	50 μ l
Injector B speed	200 μ l/s
Injection mode	Standard

3 Results and Discussion

3.1 PTP1B enzyme assay

3.1.1 Plant extracts

In the course of this work, fractions of extracts of various plants known to be used for the treatment of symptoms related to T2DM in traditional Asian medicine were tested in the PTP1B enzyme assay. The crude extracts had been tested before and identified as active in the PTP1B enzyme assay.

Selection of plants, extraction, and fractionation were conducted by cooperation partners at the University of Innsbruck (D. Steinmann/H. Stuppner) and Vienna (S. Glasl).

Leonurus sibiricus fractions

The tested extract fractions of *Leonurus sibiricus* were obtained and provided by the group of S. Glasl, Department of Pharmacognosy, University of Vienna.

The crude extract as well as some fractions of the leaves of *Leonurus sibiricus* had been tested before in the PTP1B enzyme assay by S. Pan and showed only low inhibitory activity (residual PTP1B activity >50 %) [124]. Figure 9 on the following page shows the results of the PTP1B assay for the fractions tested in the course of this work, along with UA and SOV as positive controls. Fraction Ls 70a showed the strongest inhibitory activity among the tested Ls fractions, and was able to reduce the catalytic activity of PTP1B consistently below 20 % in two independent experiments at a final test concentration of 25 µg/ml. Ls 70a was therefore further tested in the cell-based assay.

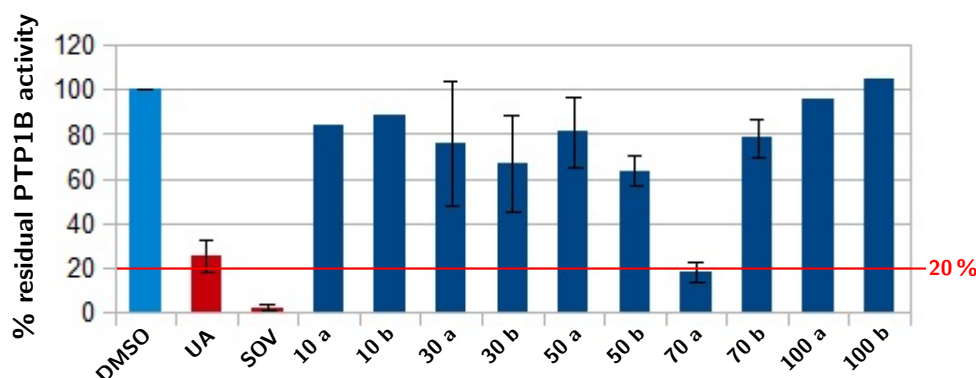


Figure 9: The effect of *Leonurus sibiricus* fractions on PTP1B activity in the PTP1B enzyme assay (test concentration 25 µg/ml). UA (30 µM) and SOV (10 µM) were used as positive controls, the DMSO control was set to 100 % enzyme activity. Samples where mean residual PTP1B activity lay below 20 % were further tested in cell-based experiments. n=1–2

Agrimonia pilosa fractions

In a previous screening, the crude methanol extract of *Agrimoniae pilosa herba*, as well as several (sub-)fractions had shown strong (residual catalytic activity of PTP1B of <20 %) inhibitory activity on PTP1B in the enzyme assay [113, 124]. The diagram in Figure 10 on the next page shows the residual activity of PTP1B in the presence of the *Agrimonia pilosa* fractions that were tested in the course of this work, in comparison to the positive controls UA and SOV. Several fractions show considerable inhibitory activity, with fraction Ah 397 (5.53 % mean residual PTP1B activity, n=2) being the most active one. For this reason, this fraction was chosen for further testing in the cell-based assay.

Terminalia nigrovenulosa fractions

As shown in Figure 11 on page 56, presence of nearly all tested *Terminalia nigrovenulosa* fractions led to a residual PTP1B activity of below 50 % in the enzyme assay. Fractions Tn 346, and especially Tn 422 and Tn 423 showed the highest inhibitory activity, reducing the residual PTP1B activity to an average of 6.71 % and below 1 %, respectively. These fractions were further tested in the cell-based assay.

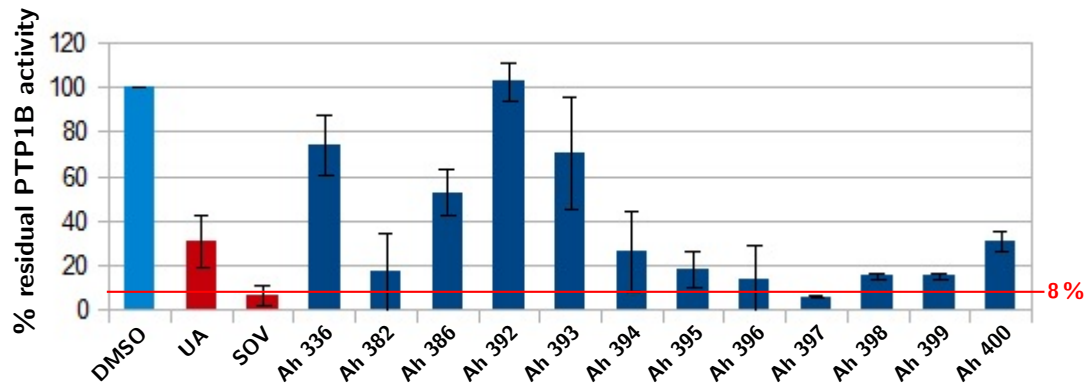


Figure 10: The effect of *Agrimonia herba pilosa* fractions on PTP1B activity in the PTP1B enzyme assay (test concentration 10 $\mu\text{g/ml}$). UA (30 μM) and SOV (10 μM) were used as positive controls, the DMSO control was set to 100 % enzyme activity. Samples where mean residual PTP1B activity lay below 8 % were further tested in cell-based experiments. $n=2-4$

Extracts of other *Terminalia* species

Figure 12 on page 57 shows a diagram with the remaining tested fractions, derived from extracts of *Terminalia bellirica*, *T. calamansanai*, and *T. citrina*. Extracts Tb 315 (*T. bellirica*) and Tci 313 (*T. citrina*) were further tested in the cell-based assay.

Summary of testing of plant extracts in the PTP1B assay

Of the 38 plant extracts tested in the PTP1B assay, only 3 (Ls 100a, Ls 100b, and Ah 392) showed no or very little activity (residual PTP1B activity $>90\%$), 12 (Ls 10a, Ls 10b, Ls 30a, Ls 30b, Ls 50a, Ls 50b, Ls 70b, Ah 336, Ah 386, Ah 393, Tn 349, and Tn 350) showed low inhibitory activity (residual PTP1B activity $>50\%$, but $<90\%$), and 6 extracts (Ah 394, Ah 400, Tn 343, Tn 344, Tn 348 and Tci 309) showed moderate inhibitory activity (residual PTP1B activity $>20\%$, but $<50\%$).

The remaining 17 fractions (Ls 70a, Ah 382, Ah 395, Ah 396, Ah 397, Ah 398, Ah 399, Tn 311, Tn 319, Tn 345, Tn 346, Tn 347, Tn 422, Tn 423, Tb 315, Tca 317, and Tci 313) showed high inhibitory activity (residual PTP1B activity $<20\%$). 7 of these extracts were able to reduce PTP1B activity below the cut-off of 20 %

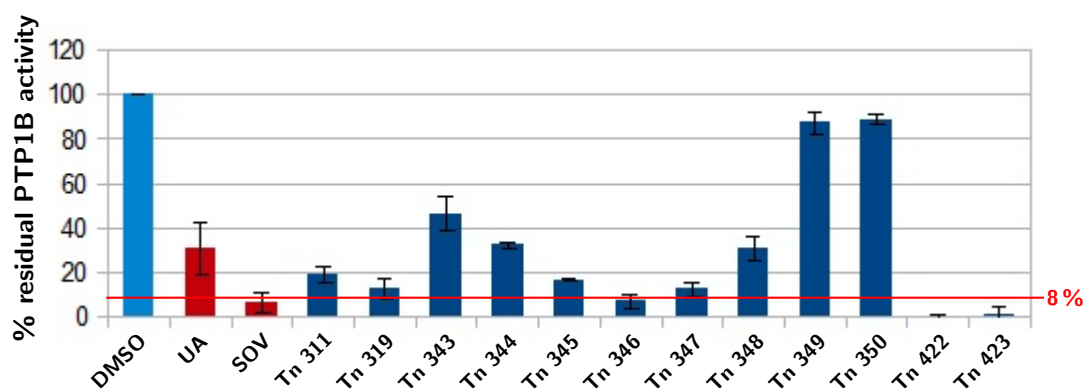


Figure 11: The effect of *Terminalia nigrovenulosa* fractions on PTP1B activity in the PTP1B enzyme assay (test concentration 10 $\mu\text{g}/\text{ml}$). UA (30 μM) and SOV (10 μM) were used as positive controls, the DMSO control was set to 100 % enzyme activity. Samples where mean residual PTP1B activity lay below 8 % were further tested in cell-based experiments. $n=2$

or 8 % (for *Leonurus sibiricus* fractions and extracts provided by D. Steinmann, respectively) in their respective test concentration, and were therefore further tested in the cell based system: Ls 70a, Ah 397, Tn 346, Tn 422, Tn 423, Tb 315, Tci 313.

3.1.2 Fatty acids

D. Steinmann et al. have identified oleic acid as the major PTP1B inhibitor in the bark of *Phellodendron amurense* (*Phellodendri amurensis* cortex) [80], a drug used in traditional chinese medicine among others against diabetes related symptoms [65]. Extracts of *Phellodendri amurensis* cortex have been shown to lower blood glucose levels in animal experiments, however, the active principle or mechanism of action were not identified [125].

During the course of this work several common C18 fatty acids with different numbers, locations and configurations of double bonds were tested for their in vitro PTP1B inhibitory activity at 1 μM , 3 μM , 10 μM and 30 μM to investigate the relationship between the structure and the PTP1B inhibitory activity of these fatty acids. From the measured residual PTP1B activity, IC_{50} values for these fatty acids were calculated (see Table 8 on page 58). Stearic acid, the fully satu-

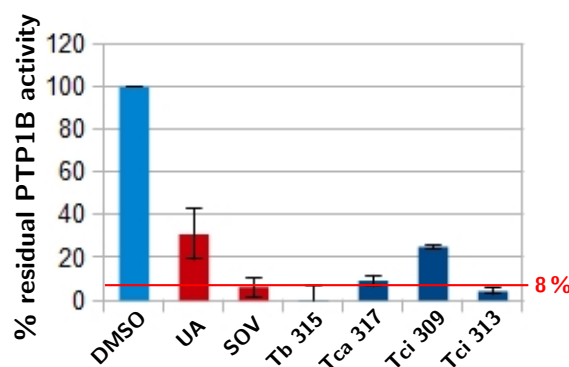


Figure 12: The effect of extracts of several *Terminalia* species on PTP1B activity in the PTP1B enzyme assay (test concentration 10 $\mu\text{g}/\text{ml}$). UA (30 μM) and SOV (10 μM) were used as positive controls, the DMSO control was set to 100 % enzyme activity. Samples where mean residual PTP1B activity lay below 8 % were further tested in cell-based experiments. n=2–4

rated C18 fatty acid, showed the highest inhibitory activity, with an IC_{50} value of 2.3 μM . For the two (*Z*)-monounsaturated C18 fatty acids petroselinic acid and oleic acid, the same IC_{50} value of 6.2 μM was measured, the bis-unsaturated linoleic acid showed activity in the same range with an IC_{50} of 6.4 μM . The tri-unsaturated linolenic acid and the (*E*)-monounsaturated vaccenic acid showed lower activity with IC_{50} values of 9.7 μM and 10.2 μM , respectively.

To sum it up, a higher number in double bonds seems to lead to a slightly decreased PTP1B inhibitory activity in C18 fatty acids, with (*E*)-configured double bonds impairing activity more strongly than (*Z*)-configured double bonds.

Table 8: Tested fatty acids, nomenclature and their IC 50 values concerning PTP1B inhibition (n=3).

Fatty acid (common name)	Nomenclature	IC50 value (μ M)
Stearic acid	Octadecanoic acid	2.3
Petroselinic acid	(6Z)-Octadec-6-enoic acid	6.2
Oleic acid	(9Z)-Octadec-9-enoic acid	6.2
Vaccenic acid	(11E)-Octadec-11-enoic acid	10.2
Linoleic acid	(9Z,12Z)-Octadecadienoic acid	6.4
α -Linolenic acid	(9Z,12Z,15Z)-Octadecatrienoic acid	9.7

3.2 Cell-based experiments related to PTP1B inhibition/insulin resistance

3.2.1 Establishment of the cell-based assay

Determination of a suitable insulin concentration

To determine which insulin concentration should be used for further experiments, serum-starved C2C12 cells were pretreated with 5 μ M SOV and then incubated with different insulin concentrations for 5 min.

As shown in Figure 13 on the next page, IR phosphorylation as well as the phosphorylation levels of Akt, ERK1/2 and GSK3 β , proteins further downstream in the insulin signalling pathway, gradually increase between 0 nM to 1000 nM. 100 nM was chosen as the concentration to be used for further cell-based experiments, because IR phosphorylation was easily detectable, but not yet at a maximum, making it possible to see increases in phosphorylation that might be caused by the test extracts.

Determination of a suitable stimulation time with insulin

To determine the incubation time that should be used for further experiments, a kinetic experiment was conducted. Serum-starved C2C12 cells were pretreated

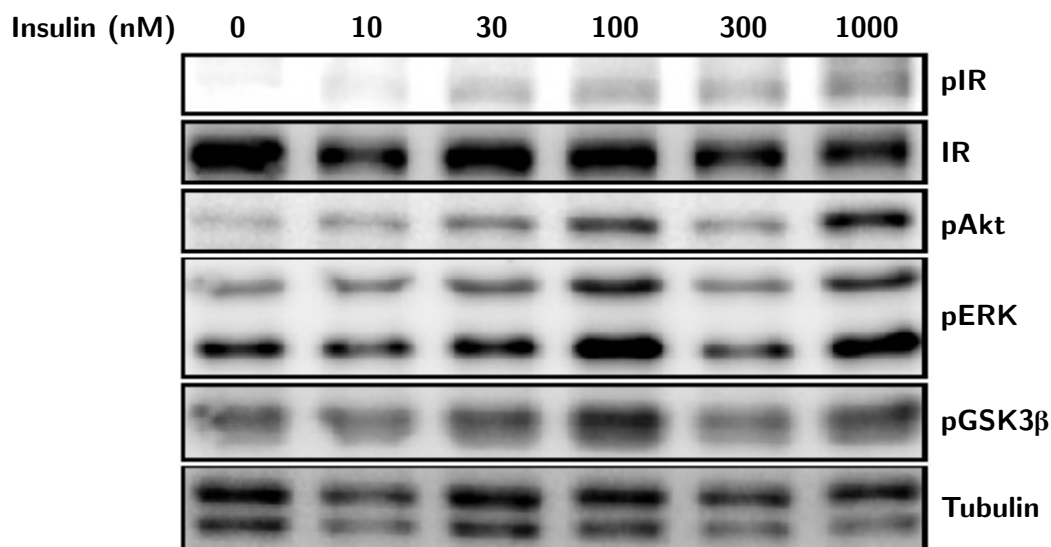


Figure 13: Western blot analysis of the phosphorylation level of IR (Tyr1150/1151) Akt (Ser473), ERK (Thr202, Tyr204) and GSK3 β (Ser9) in C2C12 myotubes after stimulation with insulin in several concentrations. Incubation time: 5 min. β -Tubulin was used as loading control. All depicted bands originate from the same membrane.

with 5 μ M SOV and then stimulated with 100 nM insulin for 0 min to 60 min.

As shown in Figure 14 on the following page, both IR and Akt phosphorylation reach a maximum at 10 min, whereas GSK3 β and ERK phosphorylation further increases until 30 min and 45 min, respectively. As the phosphorylation of IR and Akt was to be used as indicators for the potential PTP1B inhibitory activity of the test extracts, 5 min was chosen as the stimulation time for further experiments – at this point, the phosphorylation maximum is not yet reached, and more importantly, decline in phosphorylation has not yet started.

3.2.2 Cell-based assays of plant extracts

Extracts that resulted in a residual activity lower than 8 % (extracts provided by D. Steinmann) or 20 % (*Leonurus sibiricus* fractions) in their respective final test concentrations (ie. 25 μ g/ml for *Leonurus sibiricus* fractions, and 10 μ g/ml for all other extracts) in the PTP1B enzyme assay, were further tested in the cell based system using fully differentiated C2C12 muscle cells. After incubation with the extracts and (if applicable) insulin stimulation, cells were lysed, lysates separated

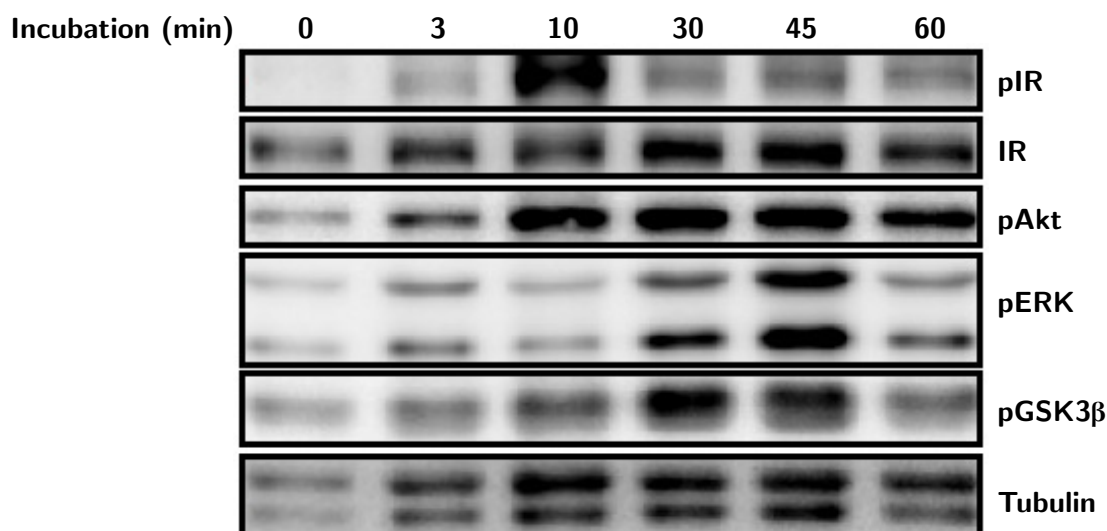


Figure 14: Western blot analysis of the time course of IR (Tyr1150/1151)-Akt (Ser473)-, ERK (Thr202/Tyr204)- and GSK3 β (Ser9)-phosphorylation in C2C12 myotubes in the presence of insulin (100 nM). β -Tubulin was used as loading control. All depicted bands originate from the same membrane.

by SDS-PAGE and proteins electrophoretically transferred on PVDF membranes, where they were detected with specific antibodies.

PTP1B inhibits insulin signal transduction by dephosphorylating the IR and its primary substrates, the IRS [44]. In cells treated with a PTP1B inhibitor, increased IR and Akt phosphorylation compared to control cells can be detected. This effect can be independent of or additive to insulin stimulation.

It should be noted here that in the used experimental setting, it is not possible to verify if any changes in IR and Akt phosphorylation can indeed be attributed solely to modulation of PTP1B.

Leonurus sibiricus fraction Ls 70a

Extract Ls 70a reduced PTP1B activity to an average of 17.75 % at a concentration of 25 μ g/ml in the enzyme assay (see Figure 9 on page 54). At the same concentration, treatment of differentiated C2C12 cells with Ls 70a resulted in a reproducibly increased IR and Akt phosphorylation in the cell-based assay (see representative blot Figure 15 on the facing page).

Using a higher concentration of extract Ls 70a for the assay did not result in

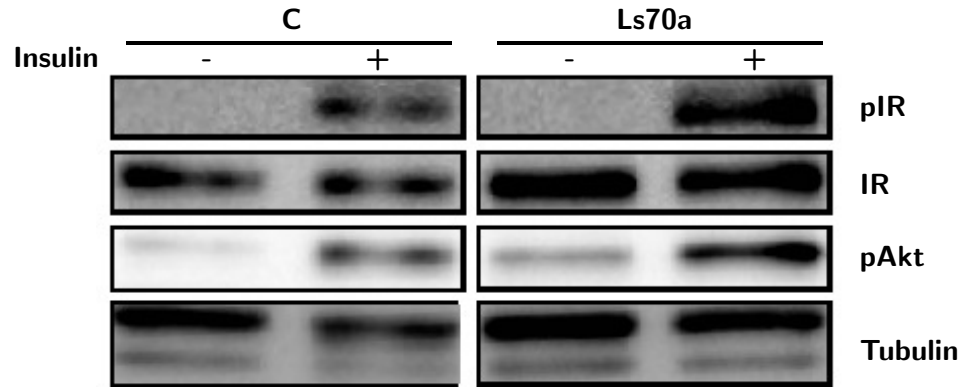


Figure 15: Western blot analysis of IR (Tyr1150/1151)- and Akt (Ser473)-phosphorylation in C2C12 myotubes after treatment with 25 µg/ml of extract Ls 70a. β-Tubulin was used as loading control. All depicted bands originate from the same membrane.

an higher increase of IR and Akt phosphorylation, as might be expected assuming a dose-dependent effect of the active principle of the extract, but instead led to decreased phosphorylation levels of both proteins compared to the DMSO-treated control cells (see Figure 16). This suggests that higher concentrations of Ls 70a impair insulin signalling or protein phosphorylation in general.

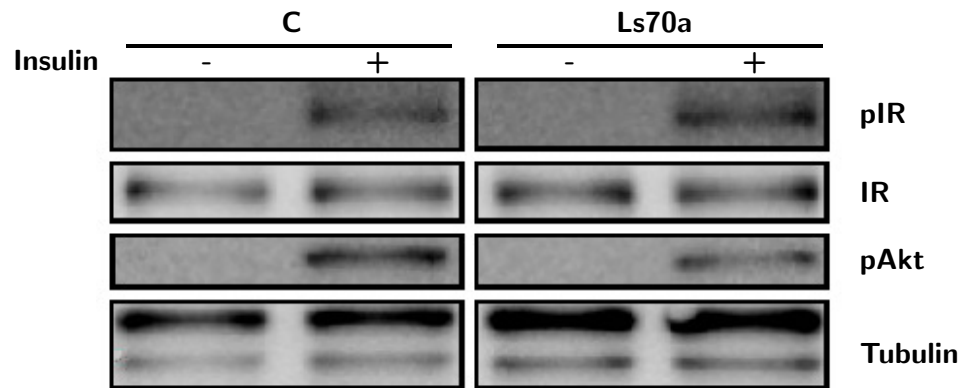


Figure 16: Western blot analysis of IR (Tyr1150/1151)- and Akt (Ser475)-phosphorylation in C2C12 myotubes after treatment with 63 µg/ml of extract Ls 70a. β-Tubulin was used as loading control. All depicted bands originate from the same membrane.

Agrimonia pilosa fraction Ah 397

As shown in Figure 10 on page 55 extract Ah 397 was able to reduce PTP1B activity to an average residual activity of 5.53 % in the PTP1B enzyme assay at a final concentration of 10 $\mu\text{g/ml}$. The representative western blot in Figure 17 shows the effects of cell treatment with Ah 397 at the same concentration compared to cells treated with corresponding amounts of DMSO. As can be seen, the phosphorylation level of IR and Akt of Ah 397 treated cells, both with and without insulin stimulation, is – if at all – only very slightly different compared to the control cells. When tested in a concentration of 30 $\mu\text{g/ml}$, Ah 397 treatment even showed a light decrease in IR and Akt phosphorylation (data not shown).

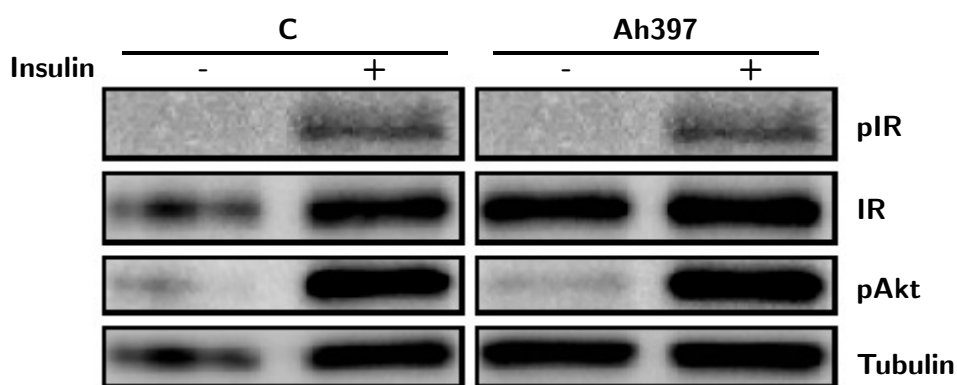


Figure 17: Western blot analysis of IR (Tyr1150/1151)- and Akt (Ser473)-phosphorylation in C2C12 cells after treatment with extract Ah 397 (test concentration: 10 $\mu\text{g/ml}$). β -Tubulin was used as loading control. All depicted bands originate from the same membrane.

Terminalia nigrovenulosa fractions Tn 346, Tn 422 and Tn 423

In the PTP1B enzyme assay, extract Tn 346 reduced PTP1B activity to an average of 6.71 %, and extracts Tn 422 and Tn 423 almost completely inhibited PTP1B (residual activity <1 %) at a concentration of 10 $\mu\text{g/ml}$ (see Figure 11 on page 56). However, all three of the extracts reproducibly (n=2) impaired IR and Akt phosphorylation at a concentration of 10 $\mu\text{g/ml}$ in the cell-based assay (for representative blots see Figures 18, 19, and 20).

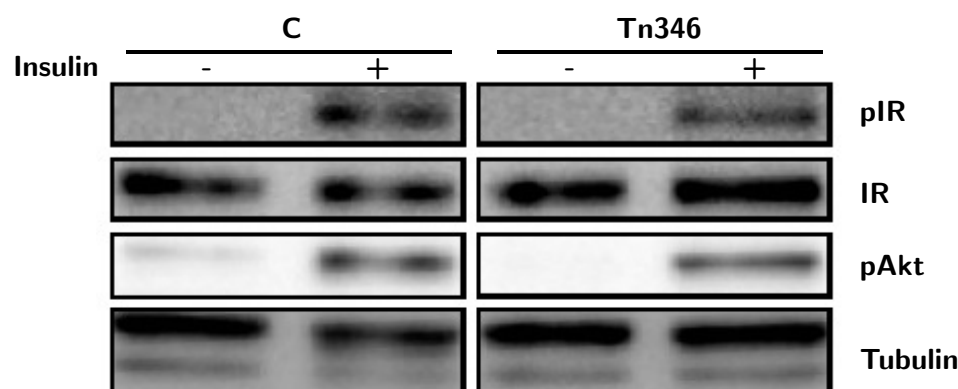


Figure 18: Western blot analysis of IR (Tyr1150/1151)- and Akt (Ser473)-phosphorylation in C2C12 myotubes after treatment with extract Tn 346 (test concentration: 10 μ g/ml). β -Tubulin was used as loading control. All depicted bands originate from the same membrane.

Terminalia bellirica fraction Tb 315

At a concentration of 10 μ g/ml extract Tb 315 reduced PTP1B activity to an average of 2.84 % in the enzyme assay (see Figure 12 on page 57). The results in the cell-based assay are somewhat contradictory: while in one of two experiments at a concentration of 10 μ g/ml an increase in Akt phosphorylation, but a decrease in IR phosphorylation could be seen (data not shown), both IR and Akt phosphorylation were left unchanged in the other experiment and when cells were treated with 30 μ g/ml Tb 315 (n=2, see representative western blot Figure 21 on page 66).

Terminalia citrina fraction Tci 313

Tci 313 reduced PTP1B activity to an average of 4.20 % at a concentration of 10 μ g/ml in the PTP1B enzyme assay (see Figure 12 on page 57). However, treatment of C2C12 cells with Tci 313 in the same concentration showed no effects on IR and Akt phosphorylation in the cell-based assay (data not shown), whereas treatment with 30 μ g/ml Tci 313 seems to negatively affect insulin signalling, leading to a decrease in IR and Akt phosphorylation (see representative blot Figure 22 on page 67).

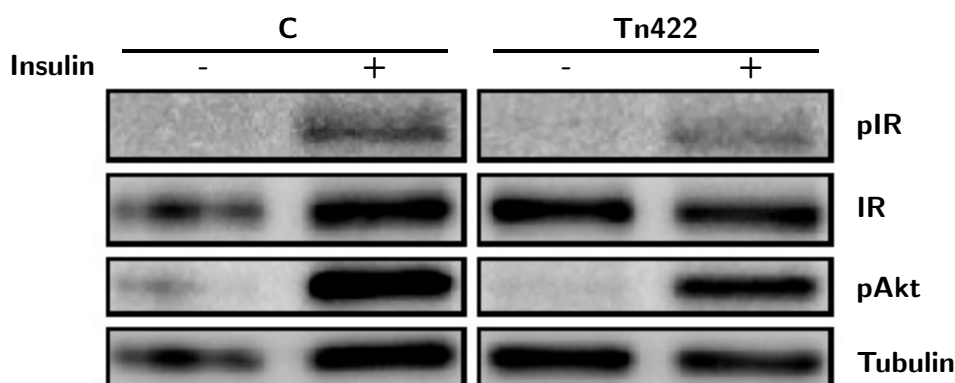


Figure 19: Western blot analysis of IR (Tyr1150/1151)- and Akt (Ser473)-phosphorylation in C2C12 myotubes after treatment with extract Tn 422 (test concentration: 10 µg/ml). β -Tubulin was used as loading control. All depicted bands originate from the same membrane.

Summary of cell-based assays of the plant extracts

Of all the extracts tested in the cell-based system, only treatment with Ls 70a at a concentration of 25 µg/mL resulted in increased IR and Akt phosphorylation, possibly due to inhibition of PTP1B. Higher concentrations of Ls 70a (63 µg/mL), as well as treatment of cells with extracts Tn 346, Tn 422, and Tn 423 (test concentration: 10 µg/mL) resulted in lower phosphorylation levels of IR and Akt compared to the DMSO control. After treatment of differentiated C2C12 cells with 10 µg/mL of extracts Ah 397, Tb 315, and Tci 313, no differences in IR or Akt phosphorylation could be detected, whereas treatment with 30 µg/mL Ah 397 and Tci 313 led to lower phosphorylation levels compared to control cells.

A reason why extracts that showed high PTP1B inhibitory activity in the enzyme assay were not able to enhance insulin signalling in the cell based system might be that the active principle could not permeate the cell membrane of the C2C12 myotubes. Many known PTP1B inhibitors are highly charged and therefore have very low membrane permeability and in consequence low bioavailability [36]. It is also conceivable that the active principle is inactivated before it reaches the place of action or that the extract influences the cells in some other way (for example by impairing protein phosphorylation) that reduces or even outweighs any positive effect on insulin signalling possibly induced by PTP1B inhibition – it seems likely that these effects are more pronounced in higher concentrations.

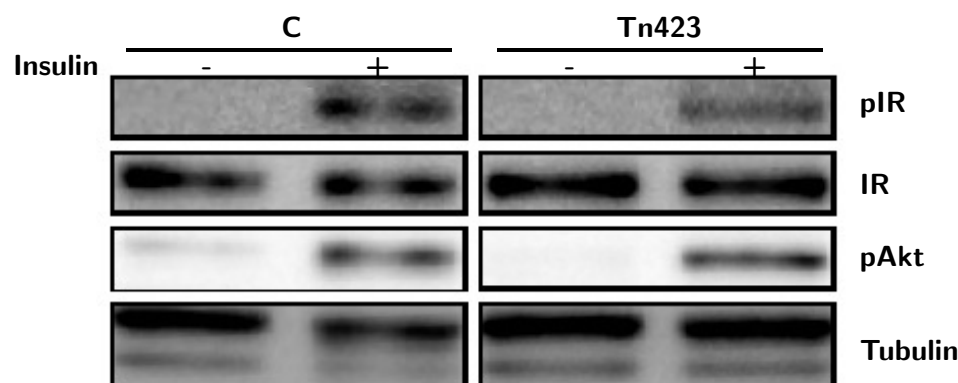


Figure 20: Western blot analysis of IR (Tyr1150/1151)- and Akt (Ser473)-phosphorylation in C2C12 myotubes after treatment with extract Tn 423 (test concentration: 10 μ g/ml). β -Tubulin was used as loading control. All depicted bands originate from the same membrane.

3.2.3 Insulin resistance model

In obesity, plasma levels of free fatty acids and inflammatory cytokines such as TNF- α are often elevated. Both of these factors have been found to contribute to impaired skeletal muscle insulin sensitivity in (pre-)diabetes, and various underlying mechanisms have been suggested (reviewed in [126]). Among other things, decreased tyrosine phosphorylation of IR and IRS-1 have been observed in insulin resistant states and obesity, along with increased expression and/or activity of PTPs, including PTP1B (summarized in [127])

Parvaneh et al. were able to show in an *in vitro* experiment that palmitate treatment results in higher PTP1B expression in C2C12 cells. Co-culture with macrophages to simulate inflammation along with palmitate treatment additively induced PTP1B overexpression [127].

For the treatment of T2DM not only direct inhibition of PTP1B is a promising strategy, but also prevention of PTP1B overexpression might be a way to overcome insulin resistance.

In order to develop the experimental setup to test compounds or extracts for their potential to reduce induction of PTP1B expression and subsequent insulin resistance, the first step was to try to show induction of PTP1B expression on protein and/or mRNA level after incubation of C2C12 cells with palmitic acid alone or together with the inflammatory cytokine TNF α . In addition, insulin responsiveness of these cells was to be examined.

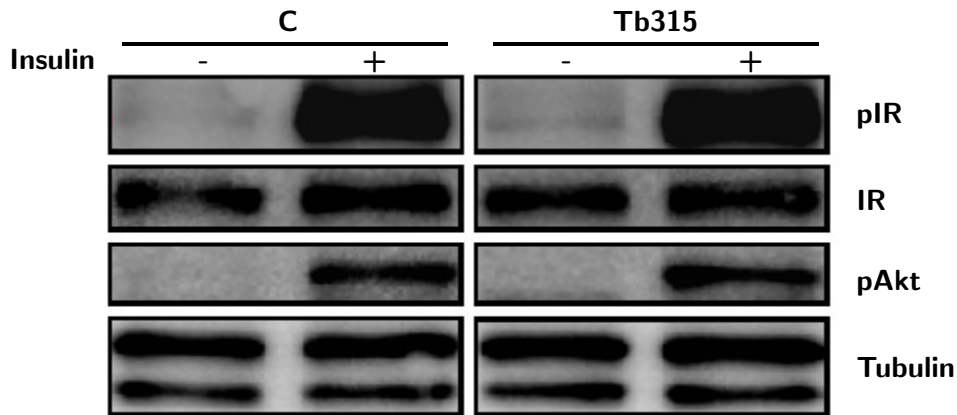


Figure 21: Western blot analysis of IR (Tyr1150/1151)- and Akt (Ser473)-phosphorylation in C2C12 myotubes after treatment with extract Tb 315 (test concentration: 30 μ g/ml). β -Tubulin was used as loading control. All depicted bands originate from the same membrane.

Results on protein level

Figure 23 shows a representative western blot of C2C12 cells treated with PA alone or together with TNF α for 21 h. One well of each group was stimulated with 100 nM insulin for 5 min at the end of the incubation time.

As can be seen, IR and Akt phosphorylation after insulin stimulation was considerably decreased in cells treated with PA compared to untreated control cells, and in cells treated with PA and TNF α compared to both control and PA only treated cells. However, detected PTP1B protein levels in all groups were the same, excluding differences of total PTP1B protein content as the reason for the obviously induced insulin resistance.

As also shown in Figure 23, the phosphorylation level of ERK, a downstream protein of the insulin signalling cascade [21], is higher in PA and PA/TNF α treated cells compared to control cells, both with and without addition of insulin to the media. This is consistent with the previous findings from cell culture experiments that TNF α and palmitate cause increased ERK 1/2 activity basally as well as following insulin stimulation [128, 129]. Also, ERK was shown to be more active in insulin resistant than in non-insulin resistant obese people [130]. This indicates that insulin resistance predominantly affects the metabolic rather than the mitogenic insulin signalling pathway.

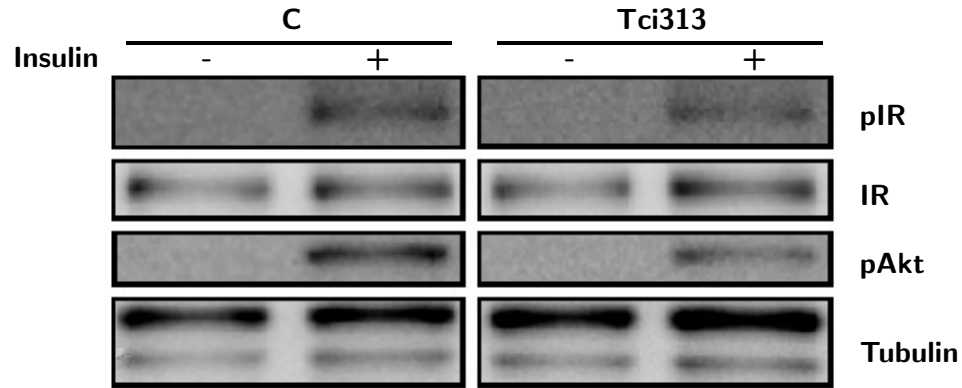


Figure 22: Western blot analysis of IR (Tyr1150/1151)- and Akt (Ser473)-phosphorylation in C2C12 myotubes after treatment with extract Tci 313 (test concentration: 30 µg/ml). β -Tubulin was used as loading control. All depicted bands originate from the same membrane.

As shown in Figure 24, treatment with PA led to a decrease of I κ B protein levels, and combination of PA and TNF α further enhanced this effect. Lower I κ B protein levels coincided with increased ERK phosphorylation (Figure 23 on the following page). This is consistent with data from Green et al., who found that exposure of skeletal muscle cells to palmitate induces NF κ B signalling in a ERK-dependent manner: activation of IKK, which phosphorylates I κ B, resulting in degradation of I κ B and activation of NF κ B, was found to be dependent on activation of ERK [131].

Results on mRNA level

To measure PTP1B mRNA levels, C2C12 cells were grown in 10 cm dishes, and, when fully differentiated, treated with PA and TNF α for 21 h. Cells were then lysed, total RNA was isolated and qPCR was conducted. mRNA levels of PTP1B and IL-6 were measured, using actin as endogenous control. Analysis was carried out using the ddCt method, mRNA levels from cells treated with the control solution were used as calibrator to calculate the relative expression levels of PTP1B and IL-6 of the PA+TNF α cells.

As shown in Figure 25 on page 69, incubation with PA and TNF resulted in an about 1.4 fold induction of PTP1B mRNA levels and in a 2.2 fold induction of IL-6 mRNA levels compared to control cells. IL-6 is an inflammatory cytokine

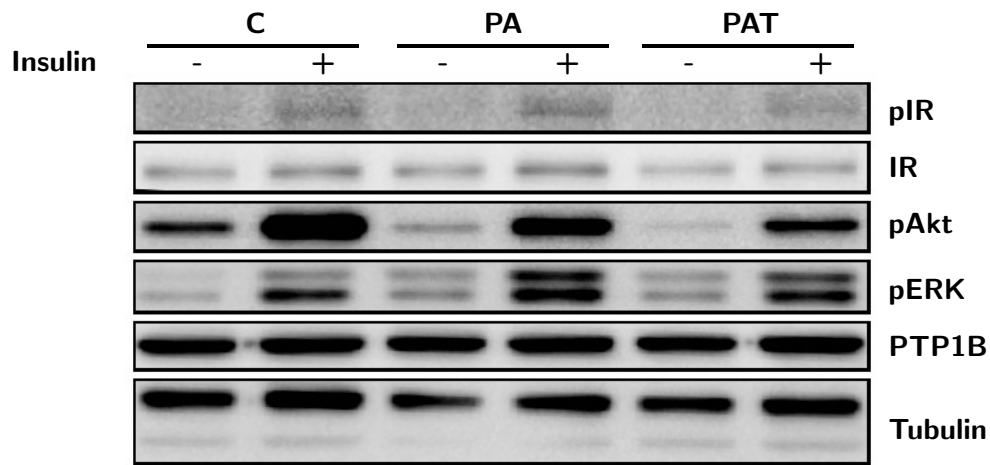


Figure 23: Western blot analysis after 21 h treatment of C2C12 cells with 0.75 mM palmitic acid alone (PA) or combined with 10 ng/mL TNF α (PAT) – with (+) or without (–) insulin stimulation (100 nM for 5 min)– of IR (Tyr1150/1151)-, Akt (Ser473)-, and ERK (Thr202/Tyr204)-phosphorylation, and PTP1B expression compared to untreated control cells (C). β -Tubulin was used as loading control. All depicted bands originate from the same membrane.

that has been shown to be induced in muscle cells by treatment with TNF α or palmitate [132, 133].

Due to lack of time, this experiment was only carried out once in the course of this work, so the presented results can only be considered as preliminary. However, they suggest that it is possible to show the effect of fatty acids and inflammatory factors observed previously by other groups [127] in the experimental setting used, and it might be possible to adapt it in order to test promising compounds/extracts for their ability to inhibit induction of PTP1B expression and inflammation by free fatty acids.

A question that remains to be solved is why no increase in PTP1B protein levels could be detected, although there was an increase of mRNA levels. A possible explanation is that it might be necessary to have a look at protein expression at a later time point than after 21 h, because it takes more time for the mRNA to be translated into the protein. Another thinkable reason is that PTP1B protein might be degraded at the same rate as newly synthesised. Moreover, insulin resistance may not necessarily be caused by an alteration of total PTP1B levels but by

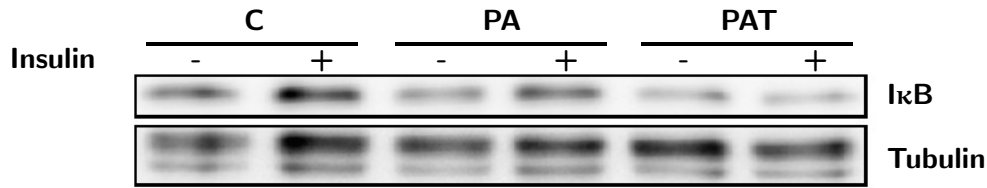


Figure 24: Western blot analysis after 21 h treatment of C2C12 cells with 0.75 mM palmitic acid alone (PA) or combined with 10 ng/mL TNFα (PAT) – with (+) or without (–) insulin stimulation (100 nM for 5 min) – of IκB expression compared to untreated control cells (C). β-Tubulin was used as loading control. All depicted bands originate from the same membrane.

an altered cellular localization of PTP1B. This could lead to different substrate specificity, as PTP1B is usually targeted to the ER membrane [43]. Nonetheless, this does not explain why an increased mRNA level is not reflected by an increased protein level. Interestingly, Stull et al. observed the same discrepancy in their study of PTP1B expression and protein content in the skeletal muscle of African American diabetics: They found PTP1B mRNA expression in the skeletal muscle of diabetics to be increased compared to non-diabetic control subjects, but did not observe any significant differences in PTP1B protein abundance between the two groups [24].

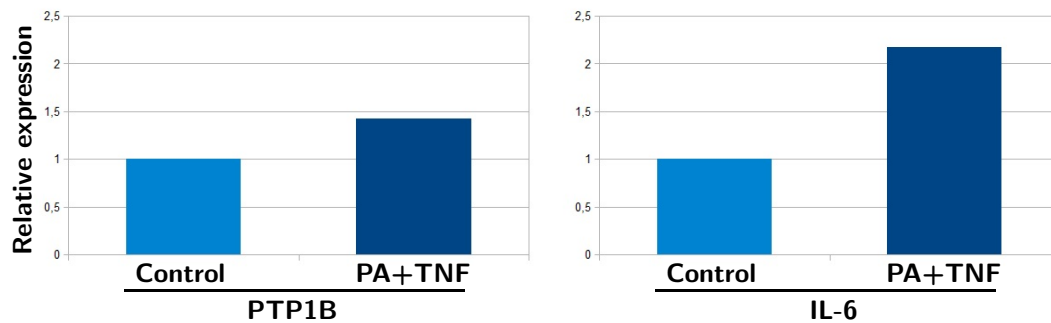


Figure 25: qPCR analysis after 21 h treatment of C2C12 myotubes with 0.75 mM palmitic acid and 10 ng/ml TNF α (PA+TNF) of the mRNA levels of PTP1B and IL-6 compared to untreated control cells (Control). Actin was used as internal control.

3.3 Cell-based experiments related to HIF-1 activation

3.3.1 Optimisation of transfection parameters

A test using different amounts and ratios of pEGFP-N1 plasmid and Fugene[®] to transfect CHO cells showed that higher amounts of plasmid DNA and Fugene[®] resulted in a higher transfection rate (see Figure 26). The best transfection rates were achieved using a transfection mix of 100 μ l OptiMEM[®], 2 μ g plasmid DNA (pEGFP-N1) and 6 or 8 μ l Fugene[®], resulting in up to 80 % transfected cells.

For the experiment conducted in the course of this work, cells were transfected using 2 μ g plasmid DNA (1.5 μ g pG13-EpoHRE-Luc and 0.5 μ g pEGFP-N1) with 8 μ l Fugene[®]. However, as with the use of only 6 μ l Fugene[®] similar results can be expected (see above), this amount should be used for future experiments in order to save Fugene[®] reagent.

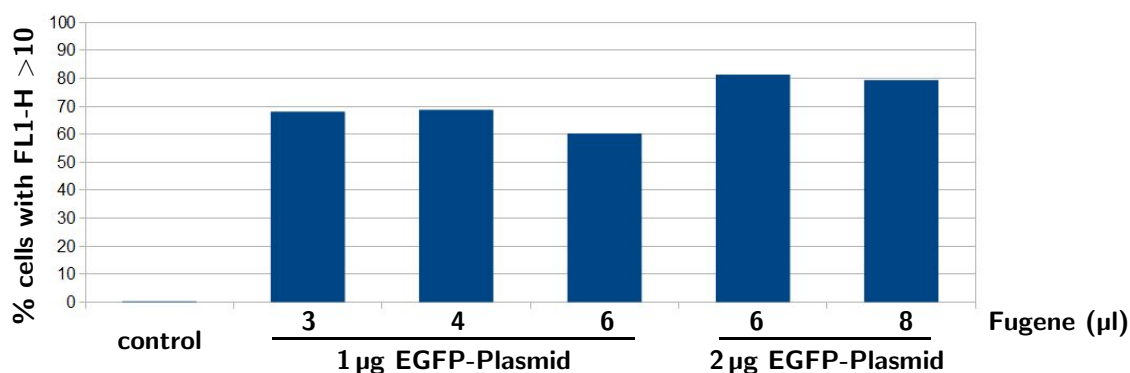


Figure 26: Flow cytometric analysis of transfection efficiency as a function of amounts of plasmid DNA and Fugene[®] present in the transfection mix. CHO cells with an FL1-H value >10 were considered as transfected successfully. Untransfected cells were used as control.

3.3.2 Luciferase assay

As shown in Figure 27, from the selected test compounds only piperine could dose-dependently induce HIF-1-dependent luciferase expression, whereas gingerol,

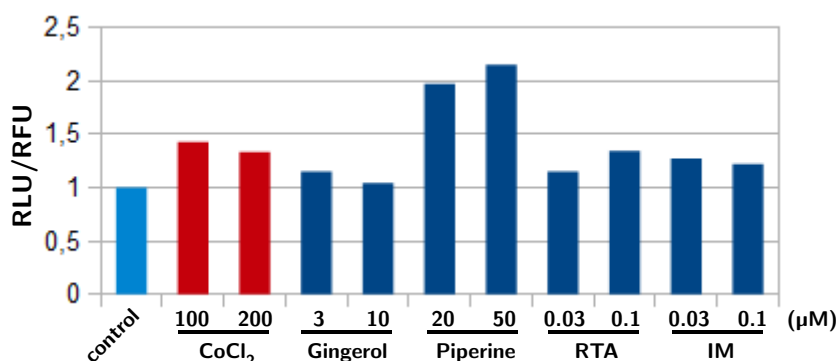


Figure 27: Luciferase reporter gene analysis of the influence of gingerol (3 μM and 10 μM), piperine (20 μM and 50 μM), RTA (0.03 μM and 0.1 μM), and IM (0.03 μM and 0.1 μM) on HIF mediated signalling. CoCl₂ (100 μM and 200 μM) was used as positive control. Respective luminescence values (RLU) were divided by EGFP-derived fluorescence values (RFU). The 0.1 % DMSO control was set to 1.

RTA, and IM failed to induce a marked increase in luciferase expression. Of note, also CoCl₂, reported in the literature as positive control when activating HIF-1α, was not able to induce HIF-1-dependent expression in our setting.

Further work is required to establish a reliable screening assay for HIF-1 activators under normoxic conditions. Especially, a properly working positive control is highly needed for this purpose.

4 Summary and Conclusion

In the course of this work, 38 fractions of extracts of 6 plants were tested for their PTP1B inhibitory activity in a colorimetric enzyme assay. Plants were selected based on their traditional use in Asia against diabetes related symptoms and subjected to bioassay-guided fractionation by cooperation partners at the Departments of Pharmacognosy at the Universities of Innsbruck and Vienna. Several fractions showed considerable activity, and the most active ones were further tested for their potential to enhance insulin signalling in a cell based system using C2C12 myotubes. Of those 7 extracts, only Ls 70a was indeed able to induce higher IR and Akt phosphorylation, in the presence and absence of insulin. However, whether or not this insulin-mimetic or -sensitizing effect is caused by PTP1B inhibition needs further investigation in a different experimental setting. Nevertheless, Ls 70a seems to be a promising source for the isolation of a modulator of the insulin response.

The other tested extracts, although potent inhibitors in the PTP1B enzyme assay, were not able to improve insulin response in the cell-based systems. This might be due to insufficient membrane permeability, a well known problem with PTP1B inhibitors, which are often very hydrophilic [36]. Nonetheless, further fractionation of the extracts found to be active in the PTP1B enzyme assay might be worthwhile, because inactivity in the cell based assay might also be caused by concurrent negative effects on insulin signalling or protein phosphorylation, along with potential PTP1B inhibition by multiple compounds still present in the fractions.

The testing of the common C18 fatty acids stearic acid, petroselinic acid, oleic acid, vaccenic acid, linoleic acid, and linolenic acid in the PTP1B assay and the calculation of their respective IC₅₀ values revealed a structure-response relationship in respect of PTP1B inhibition: Higher numbers of double bonds in fatty acids

of the same length seem to cause lower PTP1B inhibitory activity, with (*E*)-configured double bonds impairing activity more strongly than (*Z*)-configured double bonds. This knowledge might be helpful in the design of novel PTP1B inhibitors with fatty acid-like structure that may overcome the just membrane permeability problem. This part of my diploma thesis was successfully included in a recent publication [80].

Not only direct inhibition of PTP1B, but also the inhibition of PTP1B induction might be a valid strategy to prevent or overcome insulin resistance. It was therefore tried to establish an experimental set-up to simulate the insulin resistance state caused by free fatty acids and inflammation in skeletal muscle *in vitro*. After treatment of C2C12 cells with palmitate alone or in combination with TNF α , it was indeed possible to detect a decrease in phosphorylation of the IR and Akt, as well as an increase of PTP1B mRNA. Moreover, ERK phosphorylation was increased and a decrease of I κ B protein levels was found. Whether there are substances that can prevent the induction of insulin resistance by free fatty acids and inflammation remains to be investigated – the experimental set-up used here seems to be suitable for this purpose.

Some progress has been made in the attempt to establish a screening assay for HIF-1 activators under normoxic conditions. CHO cells were transfected successfully with the pGl3-EpoHRE-Luc and the pEGFP-N1 plasmid, and dose-dependent induction of HIF-1 α -dependent luciferase expression could be shown for piperine, one of the selected test compounds. However, CoCl₂, reported in the literature to stabilize HIF-1 α , did not induce luciferase expression in our setting, calling for further thorough optimization and validation of the assay.

5 References

- [1] International Diabetes Federation. The Global Burden — International Diabetes Federation, 2011. URL <http://www.idf.org/diabetesatlas/5e/the-global-burden>. visited on 31.10.2012.
- [2] Definition and diagnosis of diabetes mellitus and intermediate hyperglycemia. Report of a WHO/IDF consultation. Geneva, 2006.
- [3] Y. Handelsman and P.I S. Jellinger. Overcoming obstacles in risk factor management in type 2 diabetes mellitus. *Journal of clinical hypertension (Greenwich, Conn.)*, 13(8):613–620, 2011.
- [4] R. M. Goldenberg. Management of Unmet Needs in Type 2 Diabetes Mellitus: The Role of Incretin Agents. *Canadian Journal of Diabetes*, 35(5): 518–527, 2011.
- [5] K. G. Alberti and P. Z. Zimmet. Definition, diagnosis and classification of diabetes mellitus and its complications. Part 1: diagnosis and classification of diabetes mellitus. Report of a WHO consultation, 1999.
- [6] E. Mutschler, G. Thews, P. Vaupel, and H. Schaible. *Anatomie, Physiologie, Pathophysiologie des Menschen*. Wissenschaftliche Verlagsgesellschaft, Stuttgart, 6 edition, 2007. ISBN 9783804723429.
- [7] World Health Organization. WHO — Diabetes. URL <http://www.who.int/mediacentre/factsheets/fs312/en/index.html>. visited on 09.05.2012.
- [8] M. Stumvoll, B. J. Goldstein, and T. W. van Haeften. Type 2 diabetes: principles of pathogenesis and therapy. *Lancet*, 365(9467):1333–1346, 2005.

- [9] R. A. DeFronzo, R. C. Bonadonna, and E. Ferrannini. Pathogenesis of NIDDM. A balanced overview. *Diabetes Care*, 15(3):318–368, 1992.
- [10] G. I. Shulman. Cellular mechanisms of insulin resistance. *The Journal of clinical investigation*, 106(2):171–176, 2000.
- [11] Ralph A. Defronzo. Banting Lecture. From the triumvirate to the ominous octet: a new paradigm for the treatment of type 2 diabetes mellitus. *Diabetes*, 58(4):773–795, 2009.
- [12] S. E. Kahn, R. L. Hull, and K. M. Utzschneider. Mechanisms linking obesity to insulin resistance and type 2 diabetes. *Nature*, 444(7121):840–846, 2006.
- [13] D. M. Nathan, J. B. Buse, M. B. Davidson, R. J. Heine, R. R. Holman, R. Sherwin, and B. Zinman. Management of hyperglycemia in type 2 diabetes: A consensus algorithm for the initiation and adjustment of therapy: a consensus statement from the American Diabetes Association and the European Association for the Study of Diabetes. *Diabetes Care*, 29(8):1963–1972, 2006.
- [14] W. Harper, M. Clement, R. Goldenberg, et al. Canadian Diabetes Association 2013 Clinical Practice Guidelines for the Prevention and Management of Diabetes in Canada: pharmacologic management of type 2 diabetes. *Can J Diabetes*, 37(suppl 1):S61–S68, 2013.
- [15] European Medicines Agency. European Medicines Agency clarifies opinion on pioglitazone and the risk of bladder cancer, 21.10.2011. URL http://www.ema.europa.eu/ema/index.jsp?curl=pages/news_and_events/news/2011/10/news_detail_001368.jsp&mid=WC0b01ac058004d5c1. visited on 26.06.2013.
- [16] K. Niswender. Diabetes and obesity: therapeutic targeting and risk reduction - a complex interplay. *Diabetes, obesity & metabolism*, 12(4):267–287, 2010.
- [17] J. M. Lizcano and D. R. Alessi. The insulin signalling pathway. *Current biology : CB*, 12(7):R236–8, 2002.

- [18] M. F. White and C. R. Kahn. The insulin signaling system. *The Journal of biological chemistry*, 269(1):1–4, 1994.
- [19] S. Goetze, U. Kintscher, H. Kawano, Y. Kawano, S. Wakino, E. Fleck, W. A. Hsueh, and R. E. Law. Tumor necrosis factor alpha inhibits insulin-induced mitogenic signaling in vascular smooth muscle cells. *The Journal of biological chemistry*, 275(24):18279–18283, 2000.
- [20] P. Cohen. The twentieth century struggle to decipher insulin signalling. *Nature reviews. Molecular cell biology*, 7(11):867–873, 2006.
- [21] C. M. Taniguchi, B. Emanuelli, and C. R. Kahn. Critical nodes in signalling pathways: insights into insulin action. *Nature reviews. Molecular cell biology*, 7(2):85–96, 2006.
- [22] Q. Liu, L. Chen, L. Hu, Y. Guo, and X. Shen. Small molecules from natural sources, targeting signaling pathways in diabetes. *Biochimica et biophysica acta*, 1799(10-12):854–865, 2010.
- [23] S. Boura-Halfon and Y. Zick. Phosphorylation of IRS proteins, insulin action, and insulin resistance. *American journal of physiology*, 296(4):E581–91, 2009.
- [24] A. J. Stull, Z. Q. Wang, X. H. Zhang, Y. Yu, W. D. Johnson, and W. T. Cefalu. Skeletal muscle protein tyrosine phosphatase 1B regulates insulin sensitivity in African Americans. *Diabetes*, 61(6):1415–1422, 2012.
- [25] Y. Wei, K. Chen, A. T. Whaley-Connell, C. S. Stump, J. A. Ibdah, and J. R. Sowers. Skeletal muscle insulin resistance: role of inflammatory cytokines and reactive oxygen species. *American journal of physiology*, 294(3):R673–80, 2008.
- [26] C. Schmitz-Peiffer. Signalling aspects of insulin resistance in skeletal muscle: mechanisms induced by lipid oversupply. *Cellular Signalling*, 12(9–10):583–594, 2000.

- [27] J. E. Pessin and A. R. Saltiel. Signaling pathways in insulin action: molecular targets of insulin resistance. *The Journal of clinical investigation*, 106(2):165–169, 2000.
- [28] C. J. Bailey. Insulin resistance and antidiabetic drugs. *Biochemical Pharmacology*, 58(10):1511–1520, 1999.
- [29] A. Gastaldelli. Role of beta-cell dysfunction, ectopic fat accumulation and insulin resistance in the pathogenesis of type 2 diabetes mellitus. *Insulin: from its discovery to its role in state-of-the-art management of diabetes mellitus*, 93, Supplement 1(0):S60–S65, 2011. URL <http://www.sciencedirect.com/science/article/pii/S0168822711700158>.
- [30] V. T. Samuel and G. I. Shulman. Mechanisms for insulin resistance: common threads and missing links. *Cell*, 148(5):852–871, 2012.
- [31] G. Boden. Fatty acid-induced inflammation and insulin resistance in skeletal muscle and liver. *Current diabetes reports*, 6(3):177–181, 2006.
- [32] G. E. Bollag, R. A. Roth, J. Beaudoin, D. Mochly-Rosen, and D. E. JR Koshland. Protein kinase C directly phosphorylates the insulin receptor in vitro and reduces its protein-tyrosine kinase activity. *Proceedings of the National Academy of Sciences of the United States of America*, 83(16):5822–5824, 1986.
- [33] S. Bakhtiyari, R. Meshkani, M. Taghikhani, B. Larijani, and K. Adeli. Protein tyrosine phosphatase-1B (PTP-1B) knockdown improves palmitate-induced insulin resistance in C2C12 skeletal muscle cells. *Lipids*, 45(3):237–244, 2010.
- [34] T. Hunter. Signaling–2000 and beyond. *Cell*, 100(1):113–127, 2000.
- [35] J. Chernoff. Protein tyrosine phosphatases as negative regulators of mitogenic signaling. *Journal of cellular physiology*, 180(2):173–181, 1999.
- [36] S. Zhang and Z.-Y. Zhang. PTP1B as a drug target: recent developments in PTP1B inhibitor discovery. *Drug discovery today*, 12(9-10):373–381, 2007.

- [37] T. Mustelin, G. S. Feng, N. Bottini, A. Alonso, N. Kholod, D. Birle, J. Merlo, and H. Huynh. Protein tyrosine phosphatases. *Frontiers in bioscience : a journal and virtual library*, 7:d85–142, 2002.
- [38] N. K. Tonks. PTP1B: from the sidelines to the front lines! *FEBS letters*, 546(1):140–148, 2003.
- [39] A. Salmeen, J. N. Andersen, M. P. Myers, N. K. Tonks, and D. Barford. Molecular basis for the dephosphorylation of the activation segment of the insulin receptor by protein tyrosine phosphatase 1B. *Molecular cell*, 6(6):1401–1412, 2000.
- [40] M. P. Myers, J. N. Andersen, A. Cheng, M. L. Tremblay, C. M. Horvath, J. P. Parisien, A. Salmeen, D. Barford, and N. K. Tonks. TYK2 and JAK2 are substrates of protein-tyrosine phosphatase 1B. *The Journal of biological chemistry*, 276(51):47771–47774, 2001.
- [41] I. K. Lund. Mechanism of protein tyrosine phosphatase 1B-mediated inhibition of leptin signalling. *Journal of Molecular Endocrinology*, 34(2):339–351, 2005.
- [42] N. Dubé, A. Cheng, and M. L. Tremblay. The role of protein tyrosine phosphatase 1B in Ras signaling. *Proceedings of the National Academy of Sciences of the United States of America*, 101(7):1834–1839, 2004.
- [43] J. V. Frangioni, P. H. Beahm, V. Shifrin, C. A. Jost, and B. G. Neel. The nontransmembrane tyrosine phosphatase PTP-1B localizes to the endoplasmic reticulum via its 35 amino acid C-terminal sequence. *Cell*, 68(3):545–560, 1992.
- [44] S.-C. Yip, S. i Saha, and J. Chernoff. PTP1B: a double agent in metabolism and oncogenesis. *Trends in biochemical sciences*, 35(8):442–449, 2010.
- [45] K. Mahadev, A. Zilbering, L. Zhu, and B. J. Goldstein. Insulin-stimulated hydrogen peroxide reversibly inhibits protein-tyrosine phosphatase 1b in vivo and enhances the early insulin action cascade. *The Journal of biological chemistry*, 276(24):21938–21942, 2001.

- [46] B. P. Kennedy and C. Ramachandran. Protein tyrosine phosphatase-1B in diabetes. *Biochemical pharmacology*, 60(7):877–883, 2000.
- [47] J. N. Andersen, P. G. Jansen, S. M. Echwald, O. H. Mortensen, T. Fukada, R. Del Vecchio, N. K. Tonks, and N. P. H. Møller. A genomic perspective on protein tyrosine phosphatases: gene structure, pseudogenes, and genetic disease linkage. *FASEB journal : official publication of the Federation of American Societies for Experimental Biology*, 18(1):8–30, 2004.
- [48] M. Elchebly, P. Payette, E. Michaliszyn, W. Cromlish, S. Collins, A. L. Loy, D. Normandin, A. Cheng, J. Himms-Hagen, C. C. Chan, C. Ramachandran, M. J. Gresser, M. L. Tremblay, and B. P. Kennedy. Increased insulin sensitivity and obesity resistance in mice lacking the protein tyrosine phosphatase-1B gene. *Science (New York, N.Y.)*, 283(5407):1544–1548, 1999.
- [49] L Xie, S.-Y. Lee, J. N. Andersen, S. Waters, K. Shen, X.-L. Guo, N. P. H. Moller, J. M. Olefsky, D. S. Lawrence, and Z.-Y. Zhang. Cellular effects of small molecule PTP1B inhibitors on insulin signaling. *Biochemistry*, 42(44):12792–12804, 2003.
- [50] Z. Y. Zhang. Protein tyrosine phosphatases: prospects for therapeutics. *Current opinion in chemical biology*, 5(4):416–423, 2001.
- [51] H.-Y. Shin, S. H. Kim, S.-M. Kang, I.-J Chang, S.-Y. Kim, H. Jeon, K.-H. Leem, W.-H. Park, J.-P. Lim, and T.Y. Shin. Anti-inflammatory activity of Motherwort (*Leonurus sibiricus* L.). *Immunopharmacology and immunotoxicology*, 31(2):209–213, 2009.
- [52] G. C. de Souza, A. P. S. Haas, G. L. von Poser, E. E. S. Schapoval, and E. Elisabetsky. Ethnopharmacological studies of antimicrobial remedies in the south of Brazil. *Journal of ethnopharmacology*, 90(1):135–143, 2004.
- [53] M. A. Islam, F. Ahmed, A. K. Das, and S. C. Bachar. Analgesic and anti-inflammatory activity of *Leonurus sibiricus*. *Fitoterapia*, 76(3-4):359–362, 2005.

- [54] M.-J. Lee, H.-S. Lee, S.-D. Park, H.-I. Moon, and W.-H. Park. Leonurus sibiricus herb extract suppresses oxidative stress and ameliorates hypercholesterolemia in C57BL/6 mice and TNF- α induced expression of adhesion molecules and lectin-like oxidized LDL receptor-1 in human umbilical vein endothelial cells. *Bioscience, biotechnology, and biochemistry*, 74(2): 279–284, 2010.
- [55] E. A. Stöger. *Arzneibuch der chinesischen Medizin: Monographien des Arzneibuches der Volksrepublik China*. Dt. Apotheker-Verl, Stuttgart, 2 edition, 2012.
- [56] J. D. Keys. *Chinese herbs: Their botany, chemistry, and pharmacodynamics ; with special sections on mineral drugs, drugs of animal origin, 300 Chinese prescriptions, toxic herbs*. Swindon Book Co, Hong Kong, 1 edition, 1976. ISBN 0-8048-1179-2.
- [57] J.-P. Wang, M.-F. Hsu, and C.-M. Teng. Antiplatelet Effect of Hsien-Ho-T'sao (*Agrimonia Pilosa*). *Am. J. Chin. Med.*, 13(01n04):109–118, 1985.
- [58] K.i Miyamoto, N. Kishi, and R. Koshiura. Antitumor Effect of Agrimoniin, a Tannin of *Agrimonia pilosa* LEDEB., on Transplantable Rodent Tumors. *The Japanese Journal of Pharmacology*, 43(2):187–195, 1987.
- [59] M. Jung and M. Park. Acetylcholinesterase Inhibition by Flavonoids from *Agrimonia pilosa*. *Molecules*, 12(9):2130–2139, 2007.
- [60] L. Zhu, J. Tan, B. Wang, R. He, Y. Liu, and C. Zheng. Antioxidant Activities of Aqueous Extract from *Agrimonia pilosa* Ledeb and Its Fractions. *Chemistry & Biodiversity*, 6(10):1716–1726, 2009.
- [61] E.-K. Ahn, J. A. Lee, D.-W. Seo, S. S. Hong, and J. S. Oh. 1 β -Hydroxy-2-oxopomolic Acid Isolated from *Agrimonia pilosa* Extract Inhibits Adipogenesis in 3T3-L1 Cells. *Biological and Pharmaceutical Bulletin*, 35(5):643–649, 2012.

- [62] S.-H. Park, Y.-B. Sim, Y.-J. Kang, J.-K. Lee, S.-S. Lim, and H.-W. Suh. Effect of Agrimonia pilosa Ledeb Extract on the Antinociception and Mechanisms in Mouse. *The Korean journal of physiology & pharmacology : official journal of the Korean Physiological Society and the Korean Society of Pharmacology*, 16(2):119–123, 2012.
- [63] C.-H. Jung, J.-H. Kim, S. J. Park, D.-H. Kweon, S.-H. Kim, and S. G. Ko. Inhibitory effect of Agrimonia pilosa Ledeb. on inflammation by suppression of iNOS and ROS production. *Immunological investigations*, 39(2):159–170, 2010.
- [64] W.-J. Shin, K.-H. Lee, M.-H. Park, and B.-L. Seong. Broad-spectrum antiviral effect of Agrimonia pilosa extract on influenza viruses. *Microbiology and Immunology*, 54(1):11–19, 2010.
- [65] W. L. Li, H. C. Zheng, J. Bukuru, and N. de Kimpe. Natural medicines used in the traditional Chinese medical system for therapy of diabetes mellitus. *Journal of ethnopharmacology*, 92(1):1–21, 2004.
- [66] R. Hänsel, K. Keller, and H. Rimpler. *Drogen P - Z.: Mit 109 Arzneipflanzengattungen, 325 Arzneipflanzenarten und 752 Drogen*, volume 3. Springer-Verlag GmbH, 1994. ISBN 9783540526391.
- [67] D.-M.-C. Nguyen, D.-J. Seo, H.-B. Lee, I.-S. Kim, K.-Y. Kim, R.-D. Park, and W.-J. Jung. Antifungal activity of gallic acid purified from Terminalia nigrovenulosa bark against Fusarium solani. *Microbial pathogenesis*, 56:8–15, 2013.
- [68] D.-M.-C. Nguyen, D.-J. Seo, K.-Y. Kim, R.-D. Park, D.-H. Kim, Y.-S Han, T.-H. Kim, and W.-J. Jung. Nematicidal activity of 3,4-dihydroxybenzoic acid purified from Terminalia nigrovenulosa bark against Meloidogyne incognita. *Microbial pathogenesis*, 59-60:52–59, 2013.
- [69] A. K. Nadkarni and K. M. Nadkarni. *Indian materia medica : Dr. K. M. Nadkarni's Indian materia medica : with Ayurvedic, Unani-Tibbi, Siddha,*

- allopathic, homeopathic, naturopathic & home remedies, appendices & indexes. 1.* Bombay : Popular Prakashan, Bombay, 1994.
- [70] A. Kar, B. K. Choudhary, and N. G. Bandyopadhyay. Comparative evaluation of hypoglycaemic activity of some Indian medicinal plants in alloxan diabetic rats. *Journal of ethnopharmacology*, 84(1):105–108, 2003.
- [71] R. C. R. Latha and P. Daisy. Therapeutic potential of octyl gallate isolated from fruits of *Terminalia bellerica* in streptozotocin-induced diabetic rats. *Pharmaceutical biology*, 51(6):798–805, 2013.
- [72] M. C. Sabu and R. Kuttan. Anti-diabetic activity of medicinal plants and its relationship with their antioxidant property. *Journal of ethnopharmacology*, 81(2):155–160, 2002.
- [73] H. Makihara, T. Shimada, E. Machida, M. Oota, R. Nagamine, M. Tsubata, K. Kinoshita, K. Takahashi, and M. Aburada. Preventive effect of *Terminalia bellirica* on obesity and metabolic disorders in spontaneously obese type 2 diabetic model mice. *Journal of natural medicines*, 66(3):459–467, 2012.
- [74] S. S. Rajan and S. Antony. Hypoglycemic effect of triphala on selected non insulin dependent Diabetes mellitus subjects. *Ancient science of life*, 27(3): 45–49, 2008.
- [75] T. Tanaka, A. Morita, G.-I. Nonaka, T.-C. Lin, I. Nishioka, and F.-C. Ho. Tannins and related compounds. CIII. Isolation and characterization of new monomeric, dimeric and trimeric ellagitannins, calamansanin and calamansins A, B and C, from *Terminalia calamansanai* (Blanco) Rolfe. *Chemical and Pharmaceutical Bulletin*, 39(1):60–63, 1991.
- [76] L.-G. Chen, W.-T. Huang, L.-T. Lee, and C.-C. Wang. Ellagitannins from *Terminalia calamansanai* induced apoptosis in HL-60 cells. *Toxicology in vitro : an international journal published in association with BIBRA*, 23(4): 603–609, 2009.
- [77] A. Palasuwan, S. Soogarun, T. Lertlum, P. Pradniwat, and V. Wiwanitkit. Inhibition of Heinz body induction in an in vitro model and total antioxidant

- activity of medicinal Thai plants. *Asian Pacific journal of cancer prevention : APJCP*, 6(4):458–463, 2005.
- [78] S. Burapadaja and A. Bunchoo. Antimicrobial activity of tannins from *Terminalia citrina*. *Planta medica*, 61(4):365–366, 1995.
- [79] G. Boden. Role of fatty acids in the pathogenesis of insulin resistance and NIDDM. *Diabetes*, 46(1):3–10, 1997.
- [80] D. Steinmann, R. R. Baumgartner, E. H. Heiss, S. Bartenstein, A. G. Atanasov, V. M. Dirsch, M. Ganzera, and H. Stuppner. Bioguided Isolation of (9Z)-Octadec-9-enoic Acid from *Phellodendron amurense* Rupr. and Identification of Fatty Acids as PTP1B Inhibitors. *Planta medica*, 2011.
- [81] U. Risérus, W. C. Willett, and F. B. Hu. Dietary fats and prevention of type 2 diabetes. *Progress in Lipid Research*, 48(1):44–51, 2009.
- [82] P. P. H. Hommelberg, J. Plat, R. C. J. Langen, A. M. W. J. Schols, and R. P. Mensink. Fatty acid-induced NF-kappaB activation and insulin resistance in skeletal muscle are chain length dependent. *American journal of physiology*, 296(1):E114–20, 2009.
- [83] J. A. Chavez and S. A. Summers. Characterizing the effects of saturated fatty acids on insulin signaling and ceramide and diacylglycerol accumulation in 3T3-L1 adipocytes and C2C12 myotubes. *Archives of Biochemistry and Biophysics*, 419(2):101–109, 2003.
- [84] D. Gao, H. R. Griffiths, and C. J. Bailey. Oleate protects against palmitate-induced insulin resistance in L6 myotubes. *The British journal of nutrition*, 102(11):1557–1563, 2009.
- [85] R. H. Wenger. Cellular adaptation to hypoxia: O₂-sensing protein hydroxylases, hypoxia-inducible transcription factors, and O₂-regulated gene expression. *FASEB journal : official publication of the Federation of American Societies for Experimental Biology*, 16(10):1151–1162, 2002.

- [86] G. L. Semenza. HIF-1: mediator of physiological and pathophysiological responses to hypoxia. *Journal of applied physiology (Bethesda, Md. : 1985)*, 88(4):1474–1480, 2000.
- [87] G. L. Semenza. Hypoxia-inducible factor 1: oxygen homeostasis and disease pathophysiology. *Trends in molecular medicine*, 7(8):345–350, 2001.
- [88] C. M. Girgis, K. Cheng, C. H. Scott, and J. E. Gunton. Novel links between HIFs, type 2 diabetes, and metabolic syndrome. *Trends in endocrinology and metabolism: TEM*, 23(8):372–380, 2012.
- [89] J.-W. Lee, S.-H. Bae, J.-W. Jeong, S.-H. Kim, and K.-W. Kim. Hypoxia-inducible factor (HIF-1) α : its protein stability and biological functions. *Experimental & molecular medicine*, 36(1):1–12, 2004.
- [90] S. Rocha. Gene regulation under low oxygen: holding your breath for transcription. *Trends in biochemical sciences*, 32(8):389–397, 2007.
- [91] G. L. Semenza. Hydroxylation of HIF-1: oxygen sensing at the molecular level. *Physiology (Bethesda, Md.)*, 19:176–182, 2004.
- [92] G. L. Wang and G. L. Semenza. Desferrioxamine induces erythropoietin gene expression and hypoxia-inducible factor 1 DNA-binding activity: implications for models of hypoxia signal transduction. *Blood*, 82(12):3610–3615, 1993.
- [93] M. Y. Koh, T. R. Spivak-Kroizman, and G. Powis. HIF-1 regulation: not so easy come, easy go. *Trends in biochemical sciences*, 33(11):526–534, 2008.
- [94] Ye V. Liu, Jin H. Baek, Huafeng Zhang, Roberto Diez, Robert N. Cole, and Gregg L. Semenza. RACK1 competes with HSP90 for binding to HIF-1 α and is required for O₂-independent and HSP90 inhibitor-induced degradation of HIF-1 α . *Molecular cell*, 25(2):207–217, 2007.
- [95] Y. V. . Liu, M. E. Hubbi, F. Pan, K. R. McDonald, M. Mansharamani, R. N. Cole, J. O. Liu, and G. L. Semenza. Calcineurin promotes hypoxia-inducible factor 1 α expression by dephosphorylating RACK1 and block-

- ing RACK1 dimerization. *The Journal of biological chemistry*, 282(51):37064–37073, 2007.
- [96] D. Flügel, A. Görlach, C. Michiels, and T. Kietzmann. Glycogen synthase kinase 3 phosphorylates hypoxia-inducible factor 1 α and mediates its destabilization in a VHL-independent manner. *Molecular and cellular biology*, 27(9):3253–3265, 2007.
- [97] B. M. Emerling, F. Weinberg, J.-L. Liu, T. W. Mak, and N. S. Chandel. PTEN regulates p300-dependent hypoxia-inducible factor 1 transcriptional activity through Forkhead transcription factor 3a (FOXO3a). *Proceedings of the National Academy of Sciences of the United States of America*, 105(7):2622–2627, 2008.
- [98] G. L. Semenza. HIF-1 and human disease: one highly involved factor. *Genes & development*, 14(16):1983–1991, 2000.
- [99] D. Ochiai, N. Goda, T. Hishiki, M. Kanai, N. Senoo-Matsuda, T.i Soga, R. S. Johnson, Y. Yoshimura, and M. Suematsu. Disruption of HIF-1 α in hepatocytes impairs glucose metabolism in diet-induced obesity mice. *Biochemical and biophysical research communications*, 415(3):445–449, 2011.
- [100] E. Zelzer, Y. Levy, C. Kahana, B. Z. Shilo, M. Rubinstein, and B. Cohen. Insulin induces transcription of target genes through the hypoxia-inducible factor HIF-1 α /ARNT. *The EMBO journal*, 17(17):5085–5094, 1998.
- [101] C. Jiang, A. Qu, T. Matsubara, T. Chanturiya, W. Jou, O. Gavrilova, Y. M. Shah, and F. J. Gonzalez. Disruption of hypoxia-inducible factor 1 in adipocytes improves insulin sensitivity and decreases adiposity in high-fat diet-fed mice. *Diabetes*, 60(10):2484–2495, 2011.
- [102] X. Zhang, K. S. L. Lam, H. Ye, S. K. Chung, M. Zhou, Y. Wang, and A. Xu. Adipose tissue-specific inhibition of hypoxia-inducible factor 1{ α } induces obesity and glucose intolerance by impeding energy expenditure in mice. *The Journal of biological chemistry*, 285(43):32869–32877, 2010.

- [103] N. Zhang, Z. Fu, S. Linke, J. Chicher, J. J. Gorman, D. Visk, G. G. Haddad, L. Poellinger, D. J. Peet, F. Powell, and R. S. Johnson. The asparaginyl hydroxylase factor inhibiting HIF-1alpha is an essential regulator of metabolism. *Cell metabolism*, 11(5):364–378, 2010.
- [104] S.-B. Catrina, K. Okamoto, T. Pereira, K. Brismar, and L. Poellinger. Hyperglycemia regulates hypoxia-inducible factor-1 alpha protein stability and function. *Diabetes*, 53(12):3226–3232, 2004.
- [105] K. A. Mace, D. H. Yu, K. Z. Paydar, N. Boudreau, and D. M. Young. Sustained expression of Hif-1alpha in the diabetic environment promotes angiogenesis and cutaneous wound repair. *Wound repair and regeneration : official publication of the Wound Healing Society and the European Tissue Repair Society*, 15(5):636–645, 2007.
- [106] G. Wang, T. K. Hazra, S. Mitra, H. M. Lee, and E. W. Englander. Mitochondrial DNA damage and a hypoxic response are induced by CoCl₂ in rat neuronal PC12 cells. *Nucleic acids research*, 28(10):2135–2140, 2000.
- [107] B. H. Jiang, J. Z. Zheng, S. W. Leung, R. Roe, and G. L. Semenza. Transactivation and inhibitory domains of hypoxia-inducible factor 1alpha. Modulation of transcriptional activity by oxygen tension. *The Journal of biological chemistry*, 272(31):19253–19260, 1997.
- [108] N. S. Chandel, E. Maltepe, E. Goldwasser, C. E. Mathieu, M. C. Simon, and P. T. Schumacker. Mitochondrial reactive oxygen species trigger hypoxia-induced transcription. *Proceedings of the National Academy of Sciences of the United States of America*, 95(20):11715–11720, 1998.
- [109] A. Triantafyllou, P. Liakos, A. Tsakalof, E. Georgatsou, G. Simos, and S. Bonanou. Cobalt induces hypoxia-inducible factor-1alpha (HIF-1alpha) in HeLa cells by an iron-independent, but ROS-, PI-3K- and MAPK-dependent mechanism. *Free radical research*, 40(8):847–856, 2006.
- [110] B. Chempakam, V. A. Parthasarathy, and T. J. Zachariah. *Chemistry of*

- spices*. CABI Pub., Wallingford and UK and Cambridge and MA, 2008. ISBN 9781845934200.
- [111] J.-M. Yon, I.-J. Baek, B. J. Lee, Y. W. Yun, and S.-Y. Nam. Emodin and [6]-gingerol lessen hypoxia-induced embryotoxicities in cultured mouse whole embryos via upregulation of hypoxia-inducible factor 1 α and intracellular superoxide dismutases. *Reproductive toxicology (Elmsford, N. Y.)*, 31(4):513–518, 2011.
 - [112] K. T. Liby, M. M. Yore, and M. B. Sporn. Triterpenoids and rexinoids as multifunctional agents for the prevention and treatment of cancer. *Nature reviews*, 7(5):357–369, 2007.
 - [113] R. Baumgartner. *Virtual and real screening of natural products to find effective modulators of protein tyrosine phosphatase PTP1B*. PhD thesis, Universität Wien, 2010.
 - [114] W. Zhang, D. Hong, Y. Zhou, Y. Zhang, Q. Shen, J.-Y. Li, L.-H. Hu, and J. Li. Ursolic acid and its derivative inhibit protein tyrosine phosphatase 1B, enhancing insulin receptor phosphorylation and stimulating glucose uptake. *Biochimica et biophysica acta*, 1760(10):1505–1512, 2006.
 - [115] G. Swarup, S. Cohen, and D. L. Garbers. Inhibition of membrane phosphotyrosyl-protein phosphatase activity by vanadate. *Biochemical and biophysical research communications*, 107(3):1104–1109, 1982.
 - [116] ATCC. Product Information Sheet for ATCC CRL-1772. URL <http://www.atcc.org/attachments/25664.pdf>. visited on 11. 10. 2012.
 - [117] R. Garrett and C.M Grisham. *Biochemistry*. Brooks/Cole Publishing Company, 2010. ISBN 9780495109358.
 - [118] I. Durrant. Light-based detection of biomolecules. *Nature*, 346(6281):297–298, 1990.
 - [119] A. Roda. *Chemiluminescence and bioluminescence: Past, present and future*. Royal Society of Chemistry, Cambridge, 2010. ISBN 9781847558121.

- [120] Is your RNA intact? Methods to check RNA integrity. URL <http://www.invitrogen.com/site/us/en/home/References/Ambion-Tech-Support/rna-isolation/tech-notes/is-your-rna-intact.html>. visited on 04.07.2013.
- [121] K. J. Livak and T. D. Schmittgen. Analysis of relative gene expression data using real-time quantitative PCR and the 2(-Delta Delta C(T)) Method. *Methods (San Diego, Calif.)*, 25(4):402–408, 2001.
- [122] G. L. Wang and G. L. Semenza. Characterization of hypoxia-inducible factor 1 and regulation of DNA binding activity by hypoxia. *The Journal of biological chemistry*, 268(29):21513–21518, 1993.
- [123] Promega. Technical Bulletin: Luciferase Assay System, 2011. URL <http://www.promega.com/~media/Files/Resources/Protocols/Technical\%20Bulletins/0/Luciferase\%20Assay\%20System\%20Protocol.pdf>. visited on 28.05.2013.
- [124] S.-P. Pan. *Natural products and insulin signalling: Aspects of the metabolic syndrome ; testing in in vitro and cell bases assays*. PhD thesis, Universität Wien, 2011.
- [125] H.-J. Kim, M.-K. Kong, and Y.-C. Kim. Beneficial effects of Phellodendri Cortex extract on hyperglycemia and diabetic nephropathy in streptozotocin-induced diabetic rats. *BMB reports*, 41(10):710–715, 2008.
- [126] S. Schenk, M. Saberi, and J. M. Olefsky. Insulin sensitivity: modulation by nutrients and inflammation. *The Journal of clinical investigation*, 118(9):2992–3002, 2008.
- [127] L. Parvaneh, R. Meshkani, S. Bakhtiyari, N. Mohammadtaghvaie, S. Gorganifiruzjaee, G. Taheripak, A. Golestani, M. Foruzandeh, B. Larijani, and M. Taghikhani. Palmitate and inflammatory state additively induce the expression of PTP1B in muscle cells. *Biochemical and biophysical research communications*, 396(2):467–471, 2010.

- [128] B. W. Winston, C. A. Lange-Carter, A. M. Gardner, G. L. Johnson, and D. W. Riches. Tumor necrosis factor alpha rapidly activates the mitogen-activated protein kinase (MAPK) cascade in a MAPK kinase kinase-dependent, c-Raf-1-independent fashion in mouse macrophages. *Proceedings of the National Academy of Sciences of the United States of America*, 92(5):1614–1618, 1995.
- [129] S. Piro, E. T. Maniscalchi, A. Monello, G. Pandini, L. G. Mascali, A. M. Rabuazzo, and F. Purrello. Palmitate affects insulin receptor phosphorylation and intracellular insulin signal in a pancreatic alpha-cell line. *Endocrinology*, 151(9):4197–4206, 2010.
- [130] N. Barbarroja, R. López-Pedrerá, M. D. Mayas, E. García-Fuentes, L. Garrido-Sánchez, M. Macías-González, R. El Bekay, A. Vidal-Puig, and F. J. Tinahones. The obese healthy paradox: is inflammation the answer? *The Biochemical journal*, 430(1):141–149, 2010.
- [131] C. J. Green, K. Macrae, S. Fogarty, D. G. Hardie, K. Sakamoto, and H. S. Hundal. Counter-modulation of fatty acid-induced pro-inflammatory nuclear factor κ B signalling in rat skeletal muscle cells by AMP-activated protein kinase. *The Biochemical journal*, 435(2):463–474, 2011.
- [132] S. Gallucci, C. Provenzano, P. Mazzei, F. Scuderi, and E. Bartocioni. Myoblasts produce IL-6 in response to inflammatory stimuli. *International immunology*, 10(3):267–273, 1998.
- [133] N. J. Pilon, K. Arane, P. J. Bilan, T. T. Chiu, and A. Klip. Muscle cells challenged with saturated fatty acids mount an autonomous inflammatory response that activates macrophages. *Cell communication and signaling : CCS*, 10(1):30, 2012.

6 Appendix

List of Tables

1	Antidiabetic agents	5
2	Test extracts/compounds	19
3	Used products and supplier information	21
4	Buffers and solutions	26
5	Antibodies used for Immunodetection	34
6	qPCR protocol	47
7	Measurement parameters for Luciferase reporter gene assay	51
8	PTP1B inhibition of fatty acids (IC 50 values)	58

List of Figures

1	Pathology of T2DM and contributing factors	3
2	Insulin signal transduction	7
3	Principle of the PTP1B enzymatic assay	36
4	Pipetting scheme for PTP1B enzyme assay	37
5	Undifferentiated C2C12 cells	39
6	Fully differentiated C2C12 cells	40
7	Pipetting scheme for cell-based PTP1B inhibition experiments	41
8	Pipetting scheme for insulin resistance experiments	42

9	Effect of <i>Leonurus sibiricus</i> fractions in the PTP1B assay	54
10	Effect of Agrimonia herba pilosa fractions in the PTP1B assay . .	55
11	Effect of Terminalia nigrovenulosa fractions in the PTP1B assay .	56
12	Effect of extracts of other <i>Terminalia</i> species in the PTP1B assay	57
13	Dose-dependent effect of insulin on protein phosphorylation	59
14	Time course of protein phosphorylation in the presence of insulin	60
15	Effect of 25 µg/ml Ls 70a on IR- and Akt-phosphorylation	61
16	Effect of 63 µg/ml Ls 70a on IR- and Akt-phosphorylation	61
17	Effect of 10 µg/ml Ah 397 on IR- and Akt-phosphorylation	62
18	Effect of 10 µg/ml Tn 346 on IR- and Akt-phosphorylation	63
19	Effect of 10 µg/ml Tn 422 on IR- and Akt-phosphorylation	64
20	Effect of 10 µg/ml Tn 423 on IR- and Akt-phosphorylation	65
21	Effect of 30 µg/ml Tb 315 on IR- and Akt-phosphorylation	66
22	Effect of 30 µg/ml Tci 313 on IR- and Akt-phosphorylation	67
23	Effect of PA alone or combined with TNFα on IR-, Akt-, and ERK phosphorylation and PTP1B expression	68
24	Effect of PA alone or combined with TNFα on IκB expression . .	69
25	Effect of PA and TNFα on mRNA levels of PTP1B and IL-6 . . .	69
26	Transfection rate as a function of used amounts of plasmid DNA and Fugene®	70
27	Influence of test substances on HIF-1 mediated signalling	71

Abbreviations

ADP	Adenosine diphosphate
Ah	Fraction of Agrimonia pilosa herba extract
Akt	=PKB
ARNT	Aryl hydrocarbon Receptor Nuclear Translocator
ATP	Adenosine triphosphate
BSA	Bovine Serum Albumine
cDNA	Complementary DNA
CHO	Chinese Hamster Ovary
Cys	Cysteine
DM	Diabetes mellitus
DMSO	Dimethyl sulfoxide
DTT	Dithiothreitol
ECL	Enhanced Chemiluminescence
EDTA	Ethylenediaminetetraacetic acid
EGFP	Enhanced Green Fluorescent Protein
ERK1/2	Extracellular signal-regulated Kinases 1/2, =MAPK1
FFA	free fatty acids
FIH-1	Factor Inhibiting HIF-1
FOX	Forkhead box
GFP	Green Fluorescent Protein

GLUT4	Glucose Transporter Type 4
Grb2	Growth factor receptor-bound protein 2
GSK3	Glycogen Synthase Kinase-3
GSK3β	β -isoform of GSK
HbA1c	glycated hemoglobin
HFSD	High Fat/Sucrose Diet
HIF	Hypoxia Inducible Factor
HRE	Hypoxia responsive element
HRP	Horse radish peroxidase
HSP90	90 kDa Heat shock protein
IκB	Inhibitor of kappa B
IGF-1	Insulin-like growth factor 1
IKK	I κ B kinase
IL-6	Interleukin 6
IR	Insulin Receptor
IRS	Insulin Receptor Substrate
JAK	Janus kinase
LB	Lysogeny broth
Ls	<i>Leonurus sibiricus</i> fraction
MAPK	Mitogen Activated Protein Kinase
MOPS	3-(N-morpholino)propanesulfonic acid

mTOR	mammalian target of rapamycin
PA	Palmitic acid
pAkt	phosphorylated Akt
PBS	Phosphate Buffered Saline
PCR	Polymerase Chain Reaction
pGSK3β	phosphorylated GSK3 β
PHD	Prolyl Hydroxylase Domain protein
PI3K	Phosphoinositide-3-kinase
pIR	phosphorylated Insulin Receptor
PKB	Protein Kinase B
PKC	Protein kinase C
pNPP	para-Nitrophenylphosphate
PTP	Protein Tyrosine Phosphatase
PTP1B	Protein Tyrosine Phosphatase 1B
pTyr	phospho-Tyrosine
PVDF	Polyvinylidene fluoride
qPCR	Quantitative real time PCR
RACK1	Receptor of activated protein kinase C
RFU	Relative Fluorescence Unit
RIPA	Radioimmunoprecipitation assay
RLU	Relative Light Unit

RT	Room Temperature
SDS	Sodium dodecyl sulfate
SDS-PAGE	Sodium dodecyl sulfate polyacrylamide gel electrophoresis
SOS	<i>Son of Sevenless</i>
SOV	Sodium orthovanadate
STAT	Signal Transducer and Activator of Transcription protein
T2DM	Type 2 Diabetes mellitus
Tb	<i>Terminalia bellirica</i> fraction
TBE	Tris/Borate/EDTA
TBS-T	Tris Buffered Saline - Tween 20
Tci	<i>Terminalia citrina</i> fraction
TCM	Traditional Chinese Medicine
Tn	<i>Terminalia nigrovenulosa</i> fraction
TNFα	Tumor Necrosis Factor α
UA	Ursolic acid
VHL	Von Hippel-Lindau protein

Curriculum Vitae

Personal information

Name:	Sophie Bartenstein
Date and place of birth:	16.01.1989, Ehenbichl
Nationality:	Austrian/German

Education

10/2008 – 8/2013	Study of Pharmacy, University of Vienna
10/2007 – 9/2008	Study of Pharmacy, University of Innsbruck
6/2007	Matura (passed with distinction)
1999 – 2007	BG/BRG Reutte
1995 – 1999	Volksschule Reutte

Danksagung

Ich möchte mich sehr herzlich bei Frau Prof. Verena Dirsch dafür bedanken, dass sie mir die Möglichkeit gegeben hat, meine Diplomarbeit in ihrer Arbeitsgruppe zu machen. Ganz besonders danke ich außerdem Frau Dr. Elke Heiß für die tolle Betreuung und der gesamten Molecular Targets group für jegliche Hilfestellung und die gute Gesellschaft. Weiters möchte ich mich bei meiner Familie und meinen Freunden für ihr Verständnis und ihre Unterstützung bedanken.